1-1-2007

Characterization of electronic board material properties under impact loaDing

Ashok Kumar Ayyaswamy
University of Nevada, Las Vegas

CHARACTERIZATION OF ELECTRONIC BOARD MATERIAL PROPERTIES UNDER IMPACT LOADING

by

Ashok kumar Ayyaswamy

Bachelor of Engineering in Mechanical Engineering
University of Madras
Tamilnadu, India
2002

A thesis submitted in partial fulfillment
of the requirements for the

Master of Science in Mechanical Engineering
Department of Mechanical Engineering
Howard R. Hughes College of Engineering

Graduate College
University of Nevada, Las Vegas
December 2007

UMI Number: 1452221

INFORMATION TO USERS

UNLV
UNIVERSITY OF NEVADA LAS VEGAS

Thesis Approval

The Graduate College
University of Nevada, Las Vegas

November 20, 20 07

The Thesis prepared by

Ashok Kumar Ayyaswamy

Entitled

Characterization of Electronic Board Material Properties Under Impact Loading

is approved in partial fulfillment of the requirements for the degree of

Master of Science in Mechanical Engineering

Examination Committee Co-Chair

Examination Committee Chair

Dean of the Graduate College

Examination Committee Member

Ajith K. Roy

Examination Committee Member

Graduate College Faculty Representative

1017-53

ABSTRACT

Characterization of Electronic Board Material Properties Under Impact Loading

By

Ashok Kumar Ayyaswamy

Dr. Mohamed B. Trabia, Examination Committee Chair
Professor and Chairperson of Mechanical Engineering
University of Nevada, Las Vegas

Dr. Brendan J. O'Toole, Examination Committee Chair
Associate Professor of Mechanical Engineering
University of Nevada, Las Vegas

On-board electronics in advanced military equipment are often subjected to severe ballistic shocks and vibrations. Impact and shock to such products can cause significant functional and physical damage. Safeguarding on-board electronic sensors from such transient shocks due to ballistic impact is of concern. While several studies document material characteristics of electronic boards under quasi-static and low impact conditions, few researchers addressed the behavior of these boards under severe impact loading. This research presents the results of testing electronic boards under different strain rates to assess the effects of strain rates on modulus of elasticity of the boards. This work also outlines the finite element modeling methodology for these electronic components that are subjected to high acceleration loads that occur over extremely short time such as impact, gun firing and blast events. The results are used to suggest material models that can be used in finite element codes to accurately describe the impact behavior of these boards.

TABLE OF CONTENTS

LIST OF FIGURES

LIST OF TABLES

ACKNOWLEDGEMENTS

I would like to dedicate this work to my parents who have always been the zeal of inspiration to perform. I deeply express my sincere gratitude to my thesis advisors Dr. Mohamed B. Trabia and Dr. Brendan J. O'Toole for trusting my abilities to work on this project. Their invaluable guidance, suggestions, thoughts throughout the entire course of this research work is priceless. They have also hugely influenced my professional & personal life in many many ways.

My research work is greatly benefited by various discussions with Dr. Liu, who is also the backbone of my experimental work.

I would like to thank Dr. Ajit K Roy, Dr.Daniel Cook and Dr. Samaan G. Ladkany for their time in reviewing the prospectus, participation in defense and counseling of the thesis as committee members.

I would also like to express my sincere thanks to Srujan Babu Sridharla, Kumar Swamy Karpanan, Jagdeep Thota, Vikram Marthandham, Anand Venkatesh, Deepak Sankar Somasundaram, for their support throughout this research work and making up a good working environment at BSL.

The financial support provided by the Army Research laboratory (ARL) is thankfully acknowledged.

CHAPTER 1

RESEARCH OBJECTIVES

The objective of this research is to assess the material properties of electronic circuit boards under impact and tensile loading. Impact occurs in many commercial and military applications. For commercial applications, impact loads may be produced by transportation, operation in vehicles, operation in aircraft, dropping an electronic assembly and maintenance. In addition to the shock produced by these impact loads that are seen in commercial applications, military applications also include gunfire shock, missile acceleration, projectile launch shock, and spin-up accelerations. Electronic components subjected to high acceleration loads that occur over extremely short period of time such as impact, gun firing, and blast events, can be on the order of tens of G's (acceleration of gravity) to thousands of G's.

To predict failures, a combination of experimental and finite element analysis (FEA) results can be used. Experimental testing of electronic circuit boards should be able to measure the material properties needed to characterize the performance of boards. Considering the application of the electronic circuit board material, impact and tensile testing are the right choices to experimentally find out the material properties under various loading conditions. It is expected that the results of this research will contribute in understanding the survivability of electronic boards subjected to shock environment.

To achieve the research objectives, the effort is divided into following tasks:

1. Design the experimental set-up for impact and tensile testing of printed circuit boards (PCB).
2. Figure out the best possible ways for data acquisition during experiments.
3. Proper selection and installation of strain gages.
4. Conduct a series of experiments to study the response of these boards under impact and tensile loading.
5. Figure out a proper method to analyze the experimental data.
6. Identify solid modeling and FEA software packages that will be able to analyze this type of problem. This package should either have some programming capability or the ability to be used as a subroutine within a programming language so that it can be incorporated for future optimization work.
7. Try to model the experiments close to the ideal situation using FEA and carryout the simulation for comparing with experimental results.
8. Study sensitivity of board materials to strain rates.
9. Suggest the possibilities to improve the survivability of the material to shock environment.

CHAPTER 2

BACKGROUND AND LITERATURE REVIEW

2.1 Background Study

According to the first Shock and Vibration Symposium in 1947, mechanical shock was defined as "a sudden and violent change in the state of motion of the component parts or particles of a body or medium resulting from the sudden application of a relatively large external force, such as a blow or impact" [1]. While other definitions were proposed since then, the basic meaning of shock remains the same. Most analysts understand shock as a transient vibration. No matter how it is described or what source produced it, the effects of mechanical shock on structures and equipment produce major design problems for a wide variety of applications.

Failures of the external housing, internal electronic components, package-to-board interconnects, and liquid crystal display panels may occur as the result of impact or shock, which is confirmed by considerable reported evidence. Under these circumstances, Printed Wire Boards (PWB's) will flex significantly during the impact event and subsequent clattering. The investigation by Heaslip and Punch [2] illustrates the response of a PWB to various shock and impact scenarios through theory, numerical simulation, and experimentation. They represented a PWB as a clamped-clamped prismatic beam in a drop test scenario which predicts deflection, bending moments and strain at any point along the beam length. Their results calculated from this model showed high levels of strain at clamped edges. The values were higher than those measured experimentally and less than simulated. Their explicit finite element simulation showed high levels of strain than those predicted by the theory.

One of the most common causes of failure for portable electronic products is from drop impact. Impact and shock to such products can cause significant functional and physical damage. Lim and Low [3] examined the drop impact response of portable electronic products at different impact orientations and drop heights. These components are subjected to very large magnitude of force and accelerations during impact and are dependent on factors such as mass, impact orientation and the surface of impact. The drop impact responses examined are the impact force and the strains and level of shock induced at a PCB. A better understanding of the shock induced at the electronic components and packages in the products can assist manufacturers not only in designing better components and electronic packages but also products which are more robust and reliable to handle shock and impact loading. Therefore, one has to consider the physical ruggedness of the electronic components along with reliability to impact and shock.

Measuring shock loads on electronic boards is an expensive process. Reliability of testing under these conditions may not be assured. One of the objectives of this proposed research is to develop an FEA methodology which allows a high degree of confidence in predicted results by comparing with experimental data. A smart FEA system can allow the designer to analyze several design alternatives and various testing scenarios before creating a prototype. The proposed system can allow the user to guide and control the direction of the modeling process.

2.2 Literature Review

It is always necessary to conduct a literature review to better understand and use them as a reference. Literature related to electronic circuit boards subjected to shock loading, tensile testing and their modeling using FEA has been conducted and discussed in detail.

2.2.1 Tensile Testing of Composites

The utilization of composite materials in structural applications has prompted the need for a characterization of their behavior under quasi-static and dynamic loading conditions. To extract the material properties under axial loading, the ASTM tensile testing standard [4] is widely followed by engineers in the experimental industry. In the present study by Okoli, et al [5], tensile tests were performed on a glass epoxy laminate at different rates of strain to determine the effects of strain rate on the Poisson's ratio of the material. The findings from the experimental results suggest that Poisson's ratio is not sensitive to strain rate. Fayad, et al [6] measured the material properties of polymer composites using tensile testing and in-turn used them in FEA to predict the material behavior.

Thota [7] conducted several tensile tests on the MTS Axial/Torsional Material Test System. This machine is used in certifying failure loads of various components, under tension, compression and torsion. Conducting tensile experiments using such machine is highly desirable.

2.2.2 Test Methodology and Approach for Impact loading of Electronic Circuit Boards.

Portable electronic devices are often subjected to shock and vibration due to various types of handling, drop or shipping and, accidental misuse. Military electronic devices are often subjected to repetitive shocks (artillery fire), sudden high G loading during launching or maneuvering projectiles or ballistic impact. Dynamic loading plays a crucial role in the performance and reliability of electronic devices used in a wide range of applications. At present manufacturers of hand-held electronic devices use the JEDEC JESD22-B104-B standard for mechanical drop testing [8]. According to this standard the drop-durability of portable electronic products is quantified and ranked by the number of drops to failure. The product is held in the desired orientation on a drop carriage that is allowed to fall onto a fixed target.

Suhir [9] evaluated the nonlinear dynamic response of a flexible printed circuit board (PCB) to shock loads acting on its support contour and proposed formulas which can be helpful when choosing the appropriate PCB type, dimensions, and the most rational lay-out of the components on the board.

Varghese, et al. [10] introduced a test methodology to examine the durability of surface-mounted interconnects under impact loading when a portable electronic product is dropped. This study considers damage accumulated in interconnects in terms of local flexural strain, strain rate, acceleration and develops a consistent, accurate and generic methodology for ranking the impact durability of different surface mount interconnects technologies. Goyal and Buratynski [11] showed that even a single drop event of an electronic product can produce a complex multi-modal transient response history.

An understanding of the shock induced at different impact orientations will help in the design of more reliable and robust products. Drop test conducted by Lim, et al. [12] explains the impact behavior of several electronic devices at various impact orientations using an orientation controlled drop tester. Of interest are the strains and shock level induced around key electronic packages within each product, and the impact force. They concluded PWA strains and accelerations vary with the electronic device for the same orientation of drop. Also for the same electronic device, the printed wiring assembly (PWA) strains and accelerations vary with drop orientation. Tests conducted by Yu, et al. [13] and Juso, et al. [14] indicated that the number of cycles to failure decreases as the PWA strain and strain rate increases. In both of the above cases, the failure was in the bulk solder. Varghese and Dasgupta [15] ran impact tests on PWA's in the in-plane and out-of-plane orientations and showed that the number of impacts to failure decreased with increasing PWA strain. They also demonstrated their approach using by applying a single impact loading condition on specimens that are constrained to have no rigid body motion.

Suhir [16] proposed analytical predictive models to show that shock test could adequately mimic drop test conditions and a probabilistic approach was used to assess the effective drop height during the drop testing. Varghese and Dasgupta [17] subjected PWA's to flexural strain rate ranging from 10^{-3}/sec to 10^{1}/sec, and observed a failure site transition from the solder to the copper trace beyond a critical PWA strain rate. They used commercially available servo-hydraulic bend testing machine (Figure 2.1) and a drop tower (Figure 2.2) for their study. Their LVDT has 0mm to 100mm displacement range and 0mm/sec to 12.5mm/sec. Their drop tower is equipped with steel spheres which were dropped on the fixture holding the specimen to conduct high speed bending tests. Their sphere mass can be varied from 65 grams to 450 grams and can achieve 0 to 6m/sec by changing the sphere drop height.

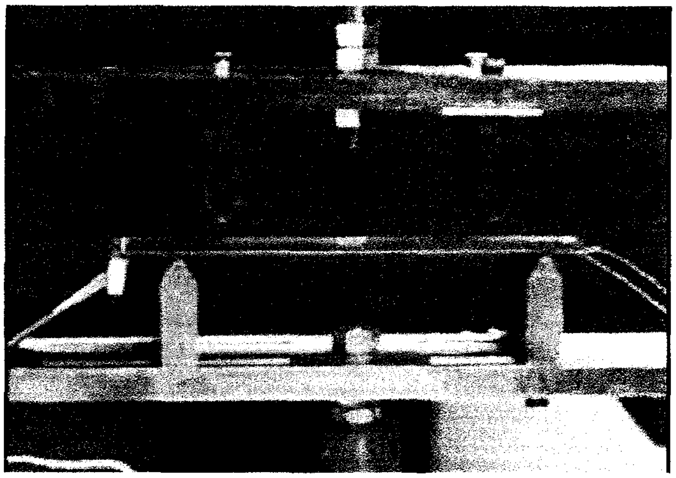

Figure 2.1: Four point bend test fixture on servo-hydraulic mechanical tester [17]

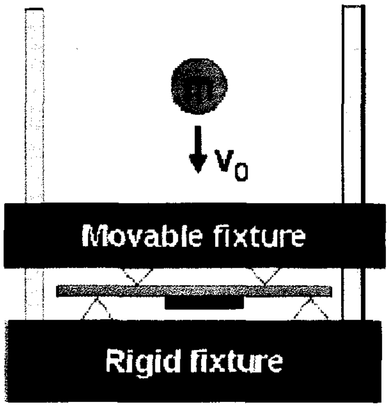

Figure 2.2: Schematic Diagram of the Ball Drop Test Setup [17]

2.2.3 Experimental Modeling of Electronic Circuit Boards Subjected to Shock/Impact

Most shock test standards, [18] and [19], including the JEDEC board-level drop impact standard [20] prescribed a half sine acceleration pulse measured on the base. They suggest that when the fundamental frequency of the test structures, namely, the base and the connectors, are significantly higher than that of the input pulse and the board, the same half sine acceleration input pulse will be transmitted to the supports of the PCB without distortion. In another words, the test structure behaves as a rigid body. In such cases, the dynamics of the board-level drop impact can be analyzed simply through application of acceleration input directly on the PCB at the supports, where it is connected to the test structure.

The dynamics of board-level drop impact can be rather simply modeled using a numerical technique, such as finite element method. This can be performed using time-integration techniques, which can be either implicit or explicit algorithms or the mode superposition technique [21] and [22]. However, the great criticism of the numerical technique is that it does not provide a fundamental understanding of the actual mechanics or physics. Wong [23] modeled the dynamic response of the PCB in a standard board-level drop impact test as a spring-mass system, a beam, and a plate. He developed analytical solutions for the time-response and amplification of the deflection, bending moment and acceleration at any point on the PCB and validated with FEA. His analysis showed that the response of PCB was dominated by the fundamental mode. It also depended heavily on the ratio between the frequency of the PCB and the input acceleration pulse. This work showed that the bending moment on the PCB is responsible for the interconnection stress, and the maximum moment and it can be most effectively reduced through reducing the PCB thickness.

Carroll, et al. [24], modeled the bending simulation of BGA SMT (Surface Mount Technology) for drop test. They modeled both in static and dynamic environments with four point bend fixtures. A known deflection was given as input for the top fixture, while the bottom rollers were fixed for the static model. An initial velocity was given to the top fixture and a zero velocity boundary condition was applied to the bottom rollers in the dynamic case. They observed higher equivalent plastic strains in dynamic bending than in static bending for the same amount of strain.

2.2.4 Failure Mechanisms in Electronic Circuit Boards due to Impact/shock loading

Seah, et al. [25] presented the results of experiments aimed at studying the effects of drop impact on portable electronics and reproducing these effects in controllable tests. They concluded that flexing of an electronic board due to direct impact is the most severe response due to the strong strain amplitudes generated. The drop/impact performance is one of important concerns in product design. Wu et al. [26] showed that portable communication devices suffer impact-induced failure. The analysis was focused at the housing break, LCD crack and structural disconnection under drop/impact shock. In this study, a finite element analysis (FEA) was also used to prove the importance of rigorous test validation. The study of "clattering" motion is important and relevant to shock protection. Goyal, et al. [27] and reported that the drop testing of an electronic product touches down first and there will be clattering as other corners strike repeatedly due to rebounds. Those cause velocity shocks at each impact, which will be several times higher than those experienced in standardized testing at a drop-table. He also addressed that clattering of the product can lead to alternating shocks that would cause resonance in suspended fragile components. Varghese and Dasgupta [28] addressed that when a product is dropped, the PWB (Printed Wiring Board) undergoes flexural deformation and the components accelerate due to inertial effects. According to them both these factors contribute to damage of interconnects. Accelerometer history of impact force alone won't provide all of the parameters required to describe impact damage. It was proposed that local flexural strain, flexural strain rate and inertial acceleration be used to describe the impact damage in interconnects. According to this study, damage is quantified in terms of structural response of the specimen, and is independent of geometry, loading and boundary conditions. Their observations indicated that for the same acceleration, as the strain increases, the damage per impact increases and hence the number of impacts to failure decreases. Similarly, damage due to impact loading depends on the rate-dependent material properties of the solder ball. Their conclusion states that the number of impacts is low for high strain rate impacts. For low strain rate impacts, the damage per impact is low, hence number of impacts to failure increases; this is represented in Figure 2.3.

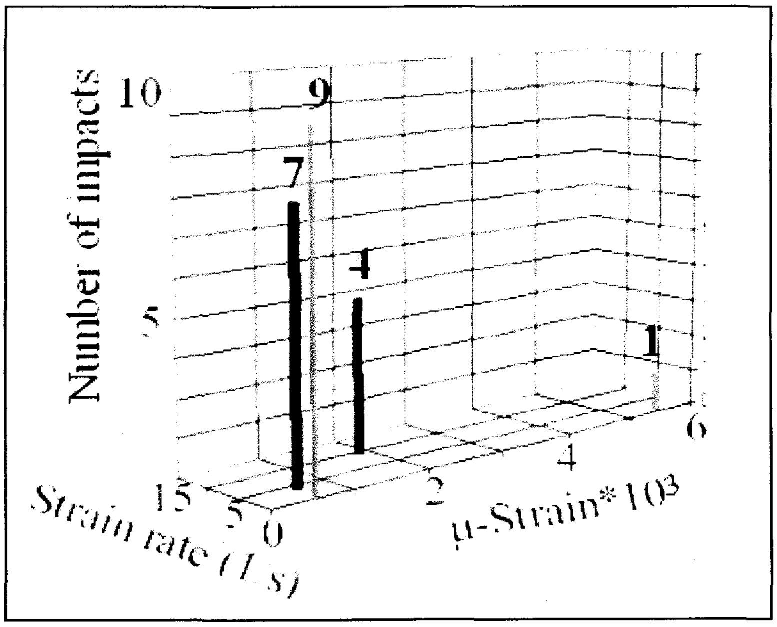

Figure 2.3: Damage as a function of PWB strain and strain rate

Shetty, et al. [29] conducted monotonic bend tests to determine the overstress curvature limits for CSP interconnects. His overstress bend test setup is as shown in

Figure 2.4. They found the average moment limit and curvature limit on the CSPs. They are considering failure as either cracking of the board or interconnect delaminating from the board which ever happens first.

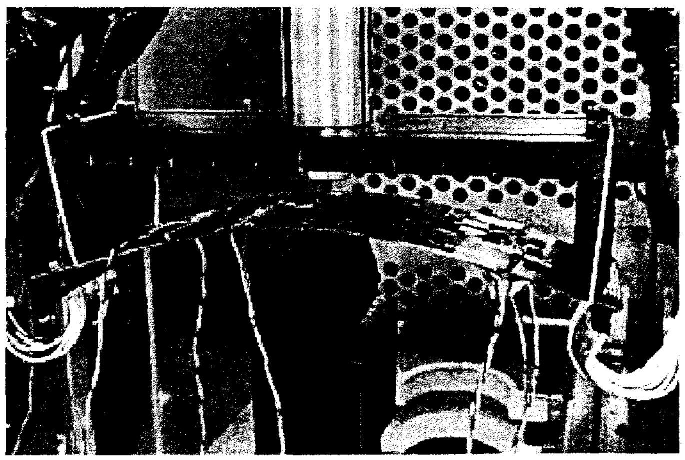

Figure 2.4: Overstress bend test

2.2.5 FEA Modeling References

Electronic boards placed inside the projectile are subjected to extremely severe loads during the launching stage. Berman, et al. [30] stated that projectiles are subjected to a quasi-static axial load in excess of 15,000 g's augmented by a transient load of up to 5000 g's. Trabia, et al. [31] developed a finite element methodology to predict the shock transmitted to electronic components within an artillery shell during the launch phase. While FEA programs and their pre-processors and post-processors have reached high levels of maturity and sophistication in their analytical capabilities, systems that can assist engineers in the critical tasks of modeling and model interpretation are not fully developed yet. Current FEA programs cannot easily evaluate the reasonableness of the assumptions that are used to create a model. They cannot readily suggest strategies for model modifications, beyond adaptive meshing. If tools for such needs are developed, they can improve the overall efficiency and reliability of analysis.

In [32], Pinfold and Chapman used knowledge-based engineering techniques to generate finite element mesh for automotive applications. They developed the knowledge-based engineering for common automotive parts. When geometry of the automotive body is imported for meshing, knowledge-based engineering simplifies the geometry for meshing according to specific rules. The authors concluded that this automated system could reduce pre-processing time significantly. Pinfold and Chapman [33] described the use of a knowledge-based engineering environment to automate the post-processing phase of the analysis. They described the stages of automating the feedback of finite element analysis results into the original design model. They selected adaptive modeling language (AML) knowledge-based engineering environment as a tool that is compatible with PATRAN and NASTRAN. The knowledge-based environment was developed to fit a family of mechanical components.

CHAPTER 3

EXPERIMENTAL PROCEDURE FOR FR4 ELECTRONIC BLANK BOARDS UNDER TENSILE LOADING

3.1 Introduction to Tensile Testing

One of the most common testing methods, tensile testing, is used to determine the behavior of a material while an axial stretching load is applied. Tensile tests are simple, relatively inexpensive, and fully standardized. By pulling on something, one can determine how the material will react to forces being applied in tension, namely the strength and elongation of the specimen. This type of testing may be performed under ambient or controlled (heating or cooling) conditions to determine the tensile properties of a material. Tensile testing is performed on a variety of materials including metals, plastics, elastomers, paper, composites, rubbers, fabrics, adhesives, films, etc.

The objective of the current research is to characterize the behavior of the electronic bland boards under shock/impact loading and measure the material properties under tensile testing. The research outlined in this thesis is used to develop practical assessment methodologies for electronic boards under mechanical shock loading and tensile testing.

3.2 Material Testing System (MTS)

All the tensile testing experiments are conducted on the MTS Axial/Torsional material test system shown in Figure 3.1. Figure 3.2 shows a scheme of the MTS layout with its primary components.

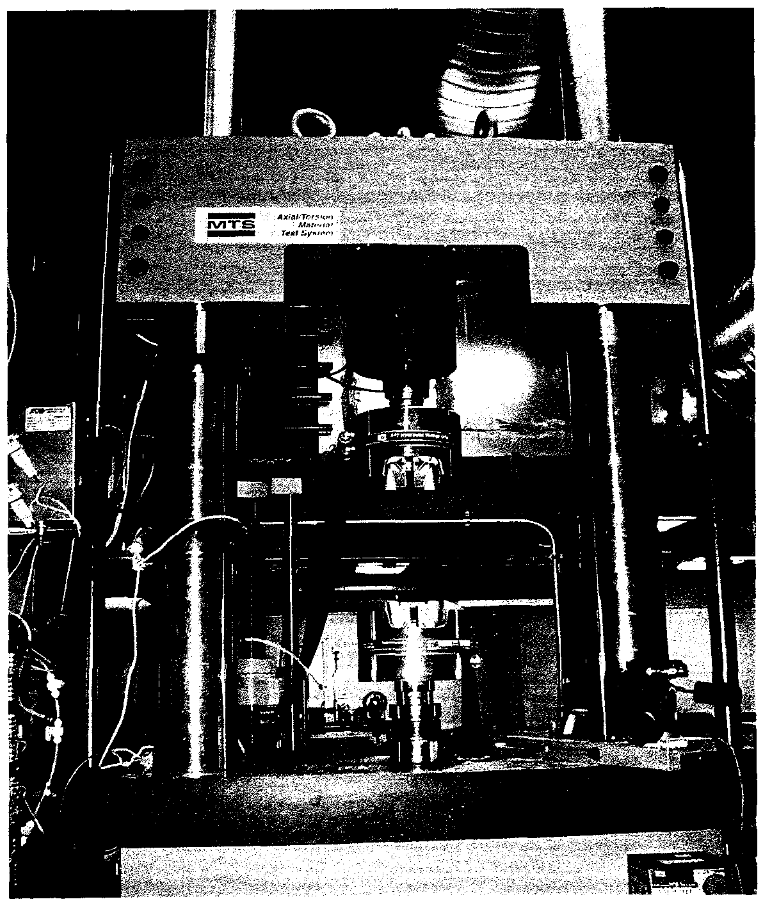

Figure 3.1: Material testing system (MTS)

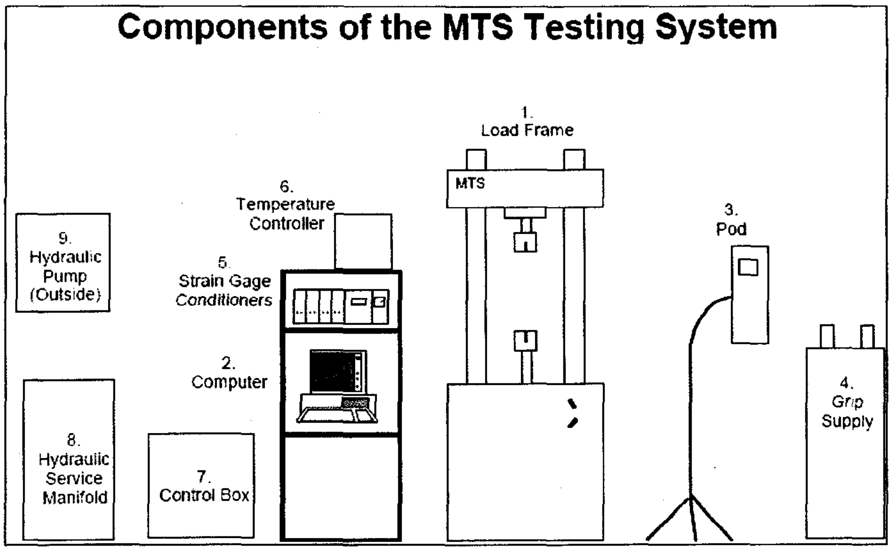

Figure 3.2: Scheme showing the MTS components

3.2.1 Load Frame

The load frame specifications of the MTS are listed in Table3.1. Figure 3.3 portrays a scheme of the load frame components in the MTS.

Table 3.1: Load frame specifications of the MTS

Working Dimensions	635 mm wide by 1463 mm high
Axial Load Transducer Limit	250 KN
Torsional Load Transducer Limit	2200 N-m
Linear Actuator Limit	± 76 mm, measured with an LVDT
Rotary Actuator Limit	100°static rotation (± 50°), measured with ADT 90° dynamic rotation (± 45°)

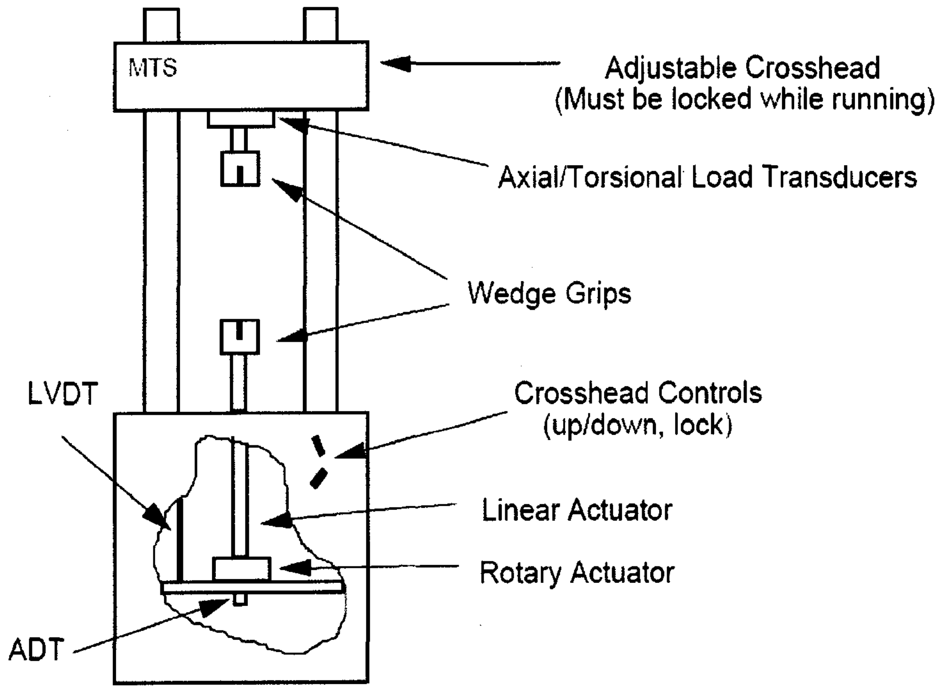

Figure 3.3: Scheme showing the load frame of the MTS

3.2.2 Computer and Software

The controlling computer is a PC system running on Windows 2000 operating system. TestStar is the main program for operating the MTS, it provides menus for activating the hydraulics to move the actuators and grip specimen. It also displays information such as displacement, angle, force, torque, strains, etc. while conducting tests on the MTS. Even test limits, such as the load limit, can be defined using the TestStar software.

3.2.3 Load Unit Control Panel (POD)

The load unit control panel or the POD is the main interface with the system for manually controlling the MTS. Figure 3.4 shows a scheme of the POD and the briefly explains the control buttons on it.

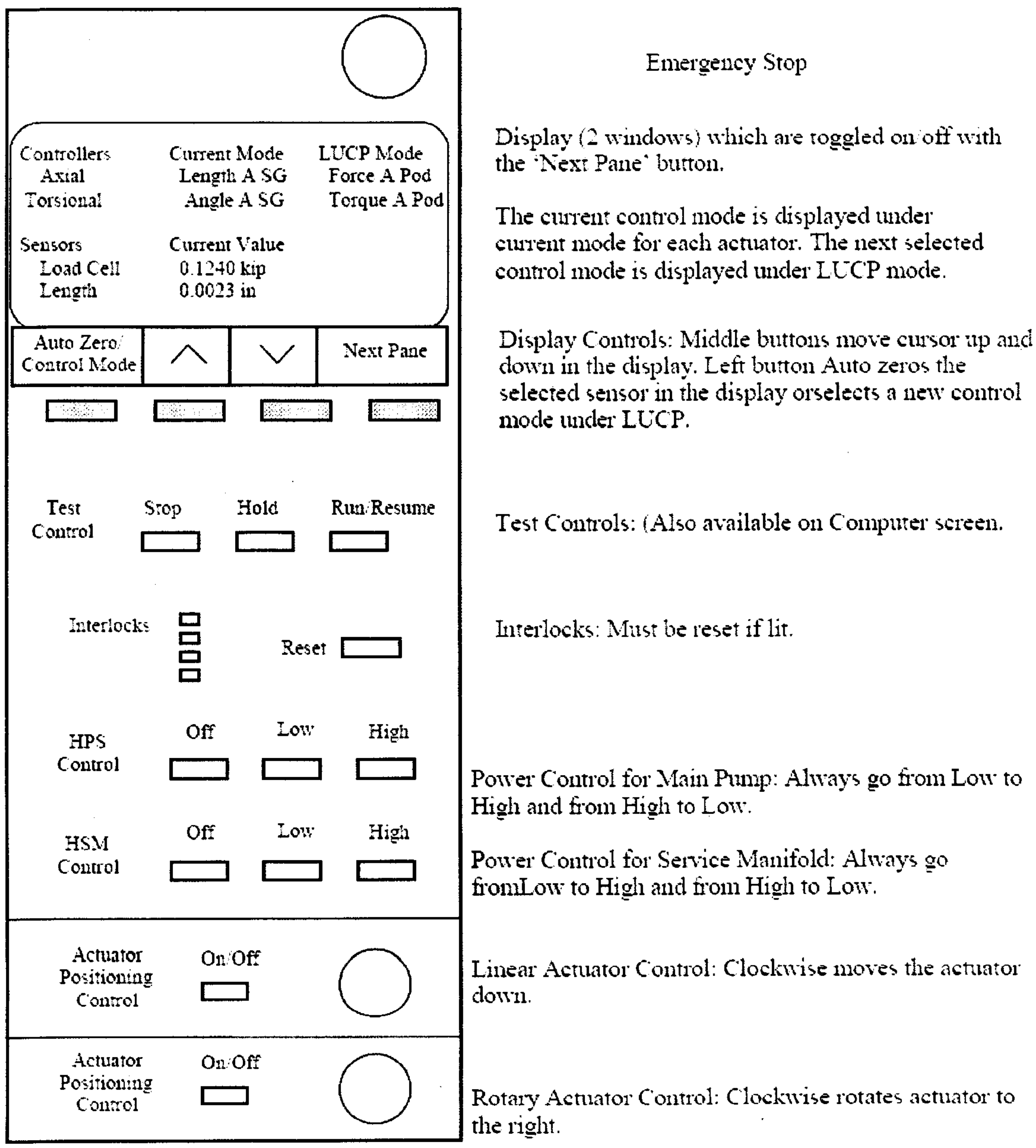

Figure 3.4: Scheme of the POD and the functions of the controls

3.2.4 Hydraulic Grip Supply

The hydraulic grip supply is used to apply gripping pressure to the specimen during a test. Gripping pressure is controlled by a combination of air and hydraulic fluid. The maximum gripping pressure of this supply unit is 45 MPa.

Wedge Grips

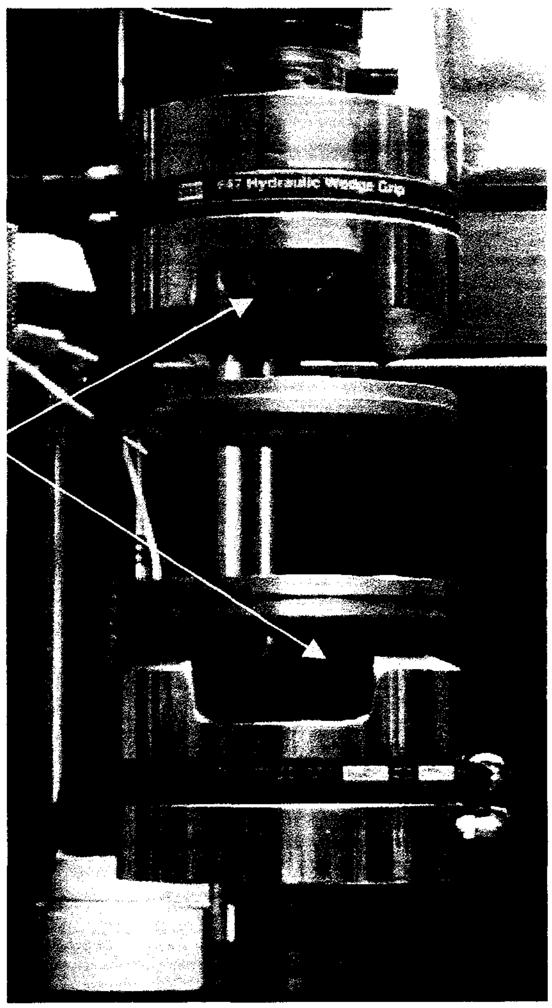

Figure 3.5: Wedge grips used for tension tests

3.2.5 Strain Gage Conditioning System

The strain gage conditioning system is used to interpret resistance change across the strain gage and convert it into micro-strain. The conditioner system on the MTS can monitor up to eight separate strain gages and report continuous strain readings to the MTS control program for data processing. But for this tension test, a separate signal conditioning amplifier is used to capture the strain signal.

3.2.6 MTS Control Unit

This box houses all the electronic signal conditioners and controllers for the hydraulic components.

3.2.7 Hydraulic Service Manifold

This unit regulates the hydraulic supply to the actuators and grip supply unit.

3.2.8 Hydraulic Pump

This is the pump and reservoir for the hydraulic system.

3.3 FR4 Test Specimen

The test specimen of concern is Flame Resistant 4 (FR4) [34] used for making printed circuit boards (PCB). FR-4 is a material from the class of epoxy resin bonded glass fabric (ERBGF). These boards are ordered as standard service boards that have top and bottom copper layers (2 layers) [34]. They do not include solder masks or silkscreen layers. Electrically, these boards are first rate with bright shiny tin/lead solder plated traces and pads. Because they do not have a green solder mask coating, the boards are the yellowish color of the industry standard FR-4 laminate.

The FR-4 used in PCBs is typically UV stabilized with a tetra functional resin system. It is manufactured strictly as an insulator and has self extinguishing flammability characteristics more suited for military applications. A PCB needs to be an insulator to avoid shorting the circuit, physically strong to protect the copper tracks placed upon it. FR-4 is preferred over cheaper alternatives such as synthetic resin bonded paper (SRBP) due to several mechanical and electrical properties; absorbs less moisture, has greater strength and stiffness and is highly flame resistant. FR-4 is widely used to build high-end consumer, industrial, and military electronic equipment. It is also ultra high vacuum (UHV) compatible. Test sample size is 228.6mm X 12.7mm X 1.42mm and prepared according to ASTM D3039-76 Standards [4] as shown in Figure 3.6.

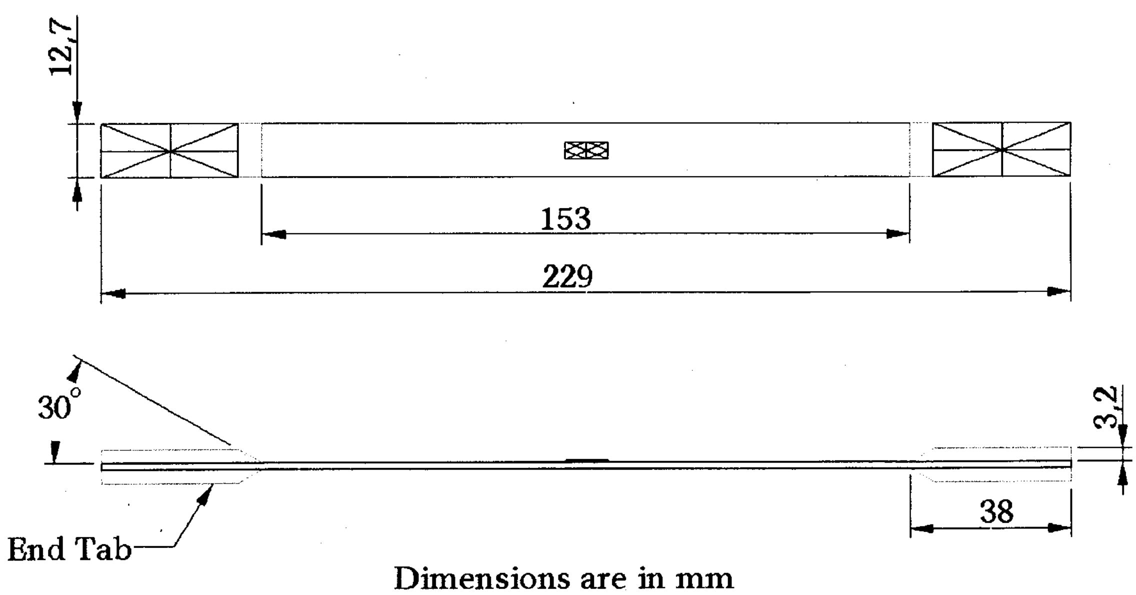

Figure 3.6: Scheme of the designed FR4 blank board specimen

The FR4 specimens are tested on the MTS machine. As the gripping pressure of the MTS machine is high enough to crush the FR4 composite material, end tabs are used to prevent this crushing and at the same time transfer the applied load into the test specimen from the loading device. Fiber-glass is used as the end tab material. The end tabs are cut to size according to the ASTM D3039-76 Standards [4] as shown in Figure 3.6. The end tabs are beveled to the required angle at one end with the help of a milling machine tool. The Fiber-glass end tabs are bonded onto the FR4 blank boards by the use of epoxy. To achieve proper alignment of end tabs to the test specimens, a mould is designed with tight tolerances as shown in Figure 3.7.

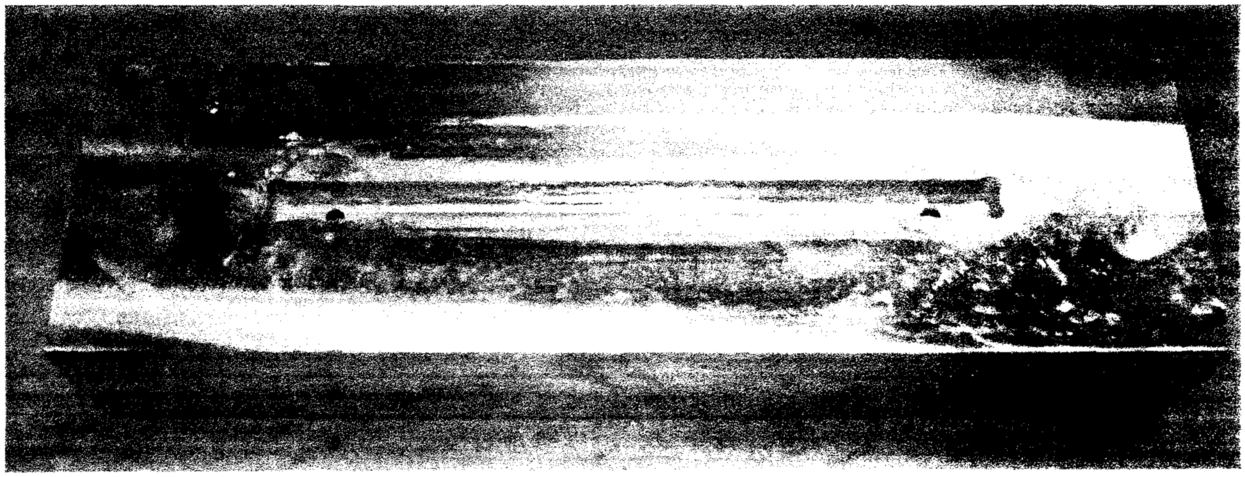

Figure 3.7: Mold for alignment of end tabs with FR4 blank board test specimens

The curing time for the test specimens inside the mold is around 12 hours and got ejected using a small pin from behind the mold. The picture of the test specimen with end tabs is shown in Figure 3.8.

Figure 3.8: FR4 blank board test specimens with end tabs

3.4 Strain Gages

Strain gages are bonded to the tension test specimens of FR4 blank boards to compute the Poisson's ratio using standard strain gage application procedures [41]. The 0-90° T-Rosette strain gage is used for obtaining the axial and transverse strains in the specimen during the test as shown in Figure 3.9. The 0-90° T-Rosette strain gages used in the static experiments have a gage factor of 2.02 and can measure strain up to a resistance of 120Ω.

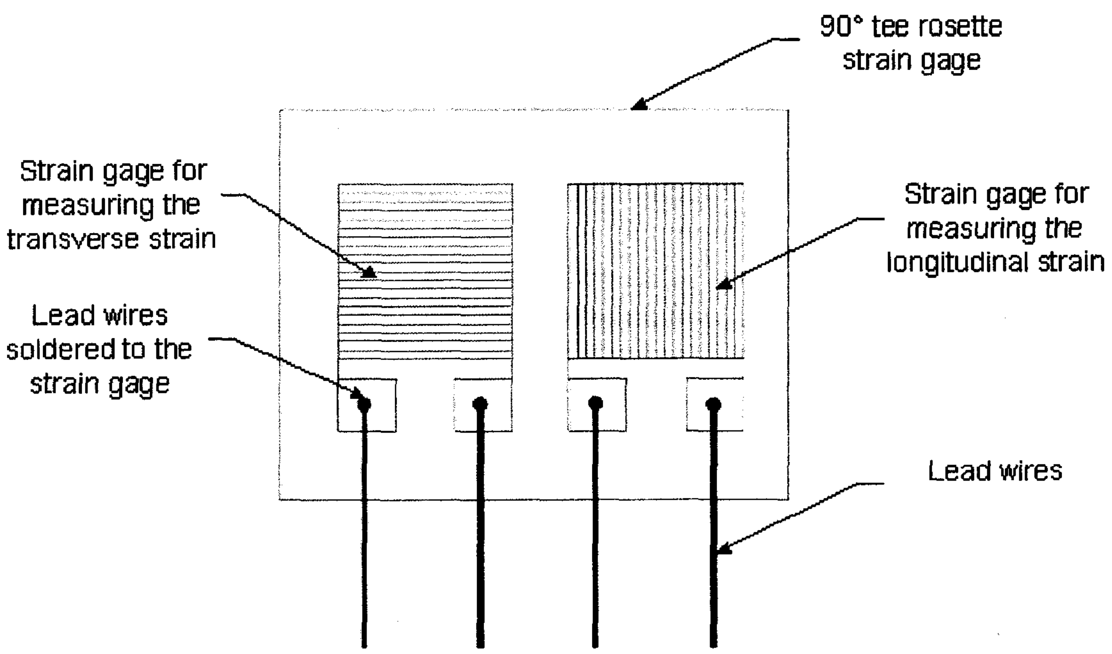

Figure 3.9: Schematic view of the 0-90° T-Rosette strain gage

3.5 Testing

Tension tests are conducted on the FR4 blank boards using the MTS machine. In order to characterize the material properties of FR4 blank boards under tension, it is decided to test the specimen under different crosshead speeds. Sridharala [35] conducted various quasi-static four point bending test on the same material. The strain rate obtained by him is used to calculate the crosshead rate of the MTS as shown in Table 3.2. The specimen is held by the wedge grips of the MTS at the end tab region as shown in Figure 3.5. The upper portion of the specimen is fixed such that it cannot move in any direction during the test. Tensile loads are applied by pulling the lower portion of the specimen in the longitudinal direction as shown in Figure 3.10.

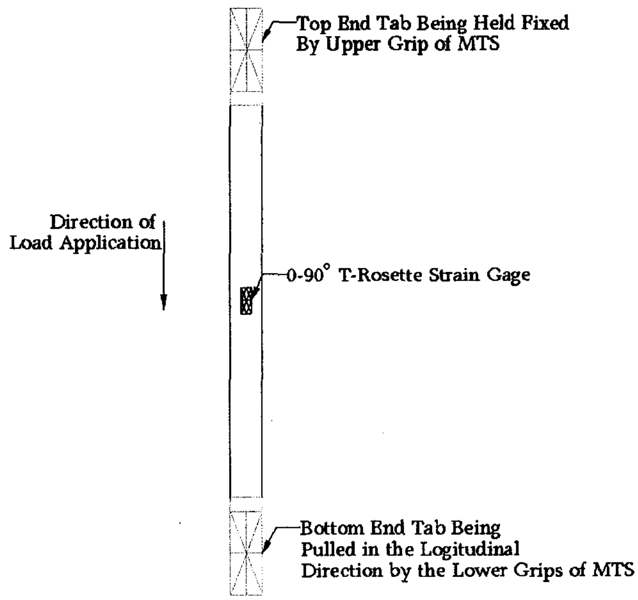

Figure 3.10: Scheme showing the application of load on FR4 blank board specimen

All specimens are tested to failure. The input crosshead speed is defined in the machine template. Lateral and longitudinal strain is measured using a signal-conditioning amplifier. The data acquisition system is the same as used for four point bending experiments, which is described in detail in Chapter 4. Test specimen after failure is shown in Figure 3.11.

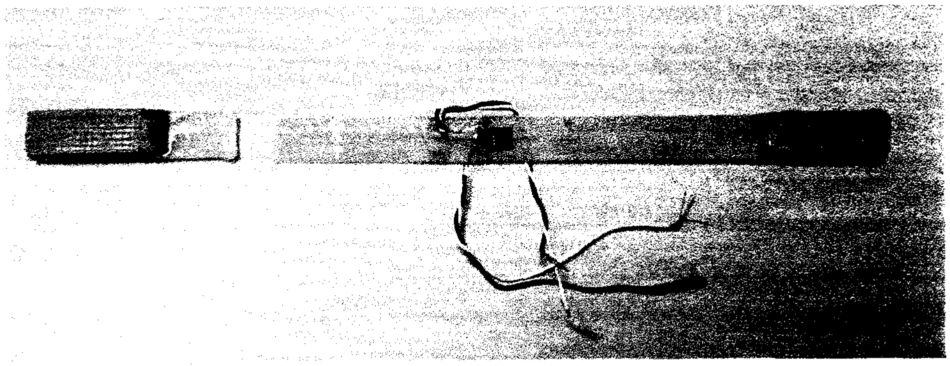

Figure 3.11: FR4 blank board specimen after pulled to failure

3.6 Experimental Results for Tensile Testing

Three samples are tested for each crosshead speed in order to check the repeatability of the test. Testing is conducted at various crosshead speeds as described in Table 3.2. The force vs. time plots is shown in Figure 3.12 through Figure 3.14. Poisson's ratio plots are shown in Figure 3.15 through Figure 3.17. Failure strain and tensile strength are found out from stress strain plots from Figure 3.19 through Figure 3.21. Strain gage on sample 2 for crosshead speed 0.244 mm/sec did not work so this sample is eliminated from material properties calculation.

Table 3.2: Test matrix for FR4 blank board

Description	Tensile Testing		
Rate of Crosshead Motion (mm/sec)	0.0244	0.244	2.44
Number of Blank Boards	3	3	3
Predicted Strain Rate(1/sec)	1.6e-4	1.6e-3	1.6e-2
Actual Strain Rate(1/sec)	1.34e-4	1.33e-3	1.1e-2

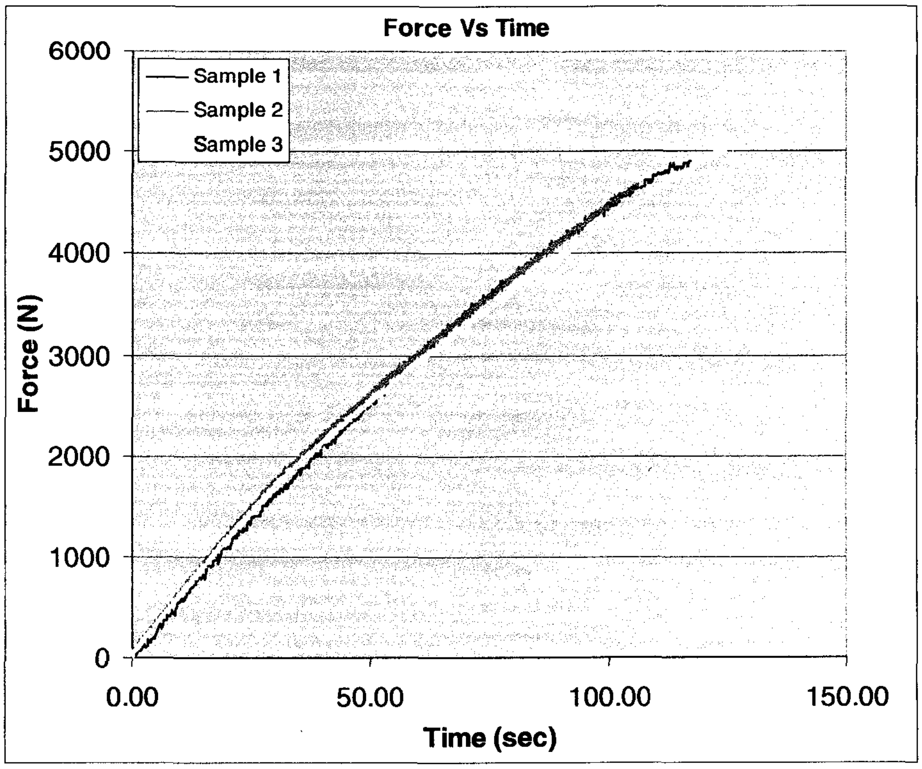

Figure 3.12 FR4 blank boards at crosshead speed of 0.0244 mm/sec

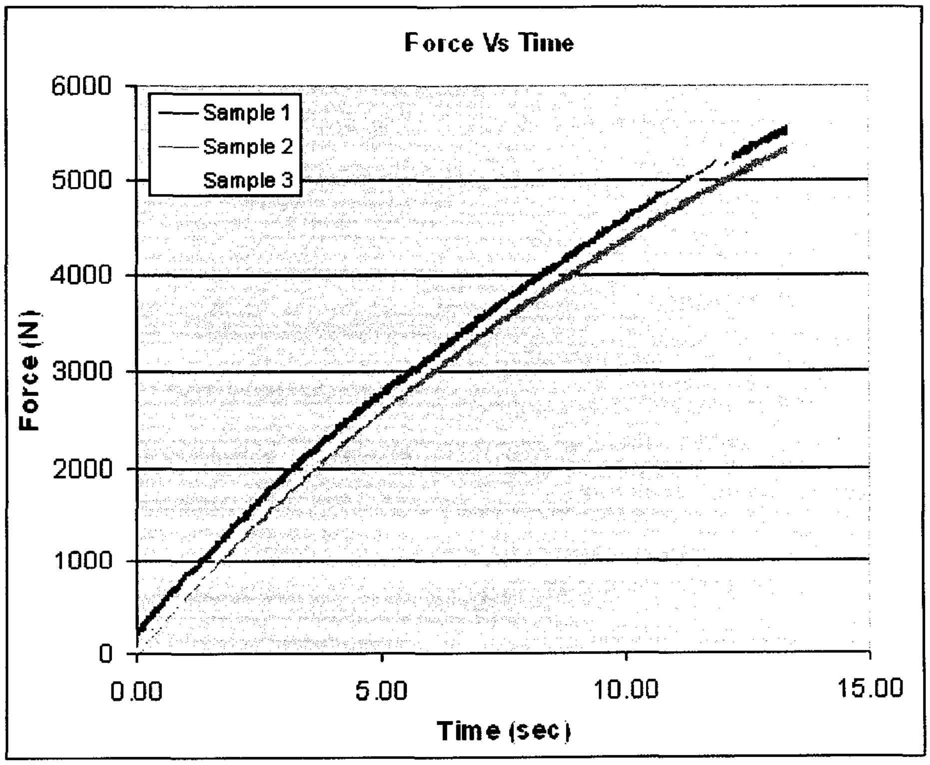

Figure 3.13 FR4 blank boards at crosshead speed of 0.244 mm/sec

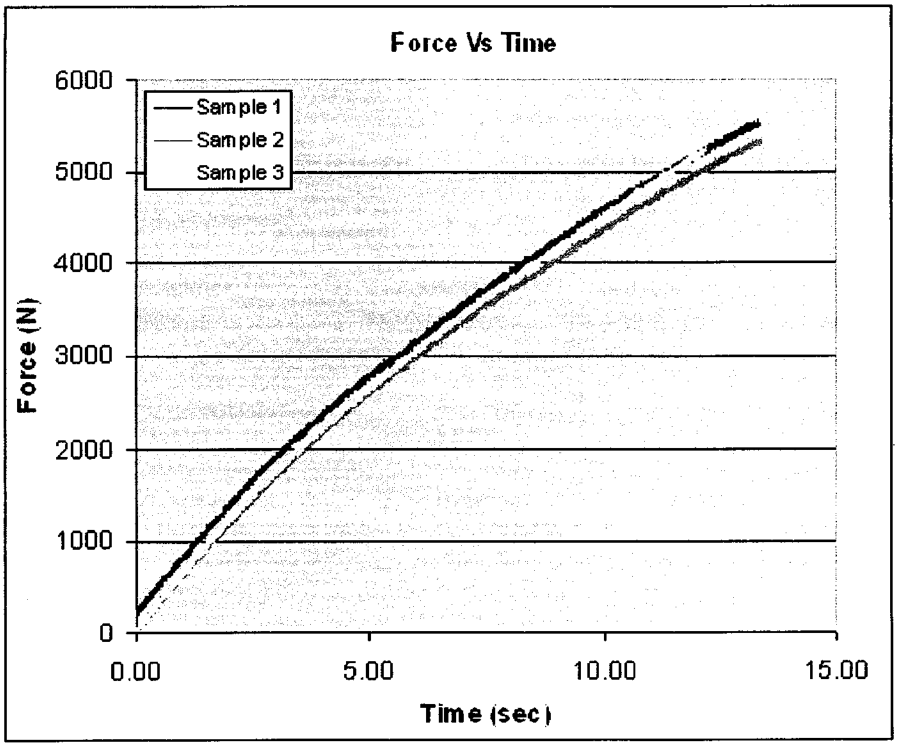

Figure 3.14 FR4 blank boards at crosshead speed of 2.44 mm/sec

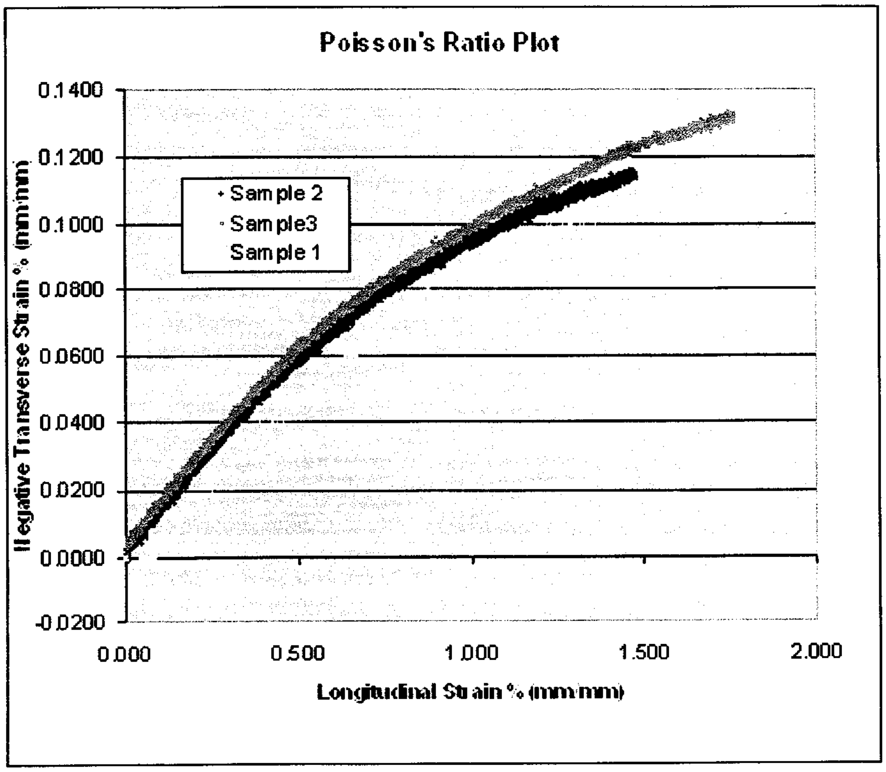

Figure 3.15 FR4 blank boards at crosshead speed of 0.0244 mm/sec

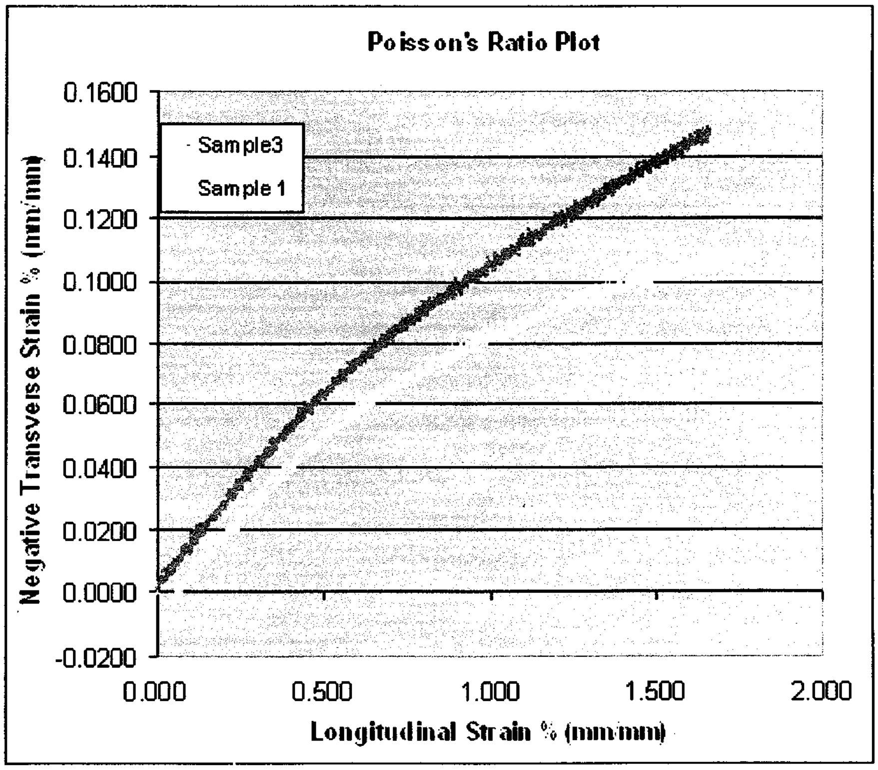

Figure 3.16 FR4 blank boards at crosshead speed of 0.244 mm/sec

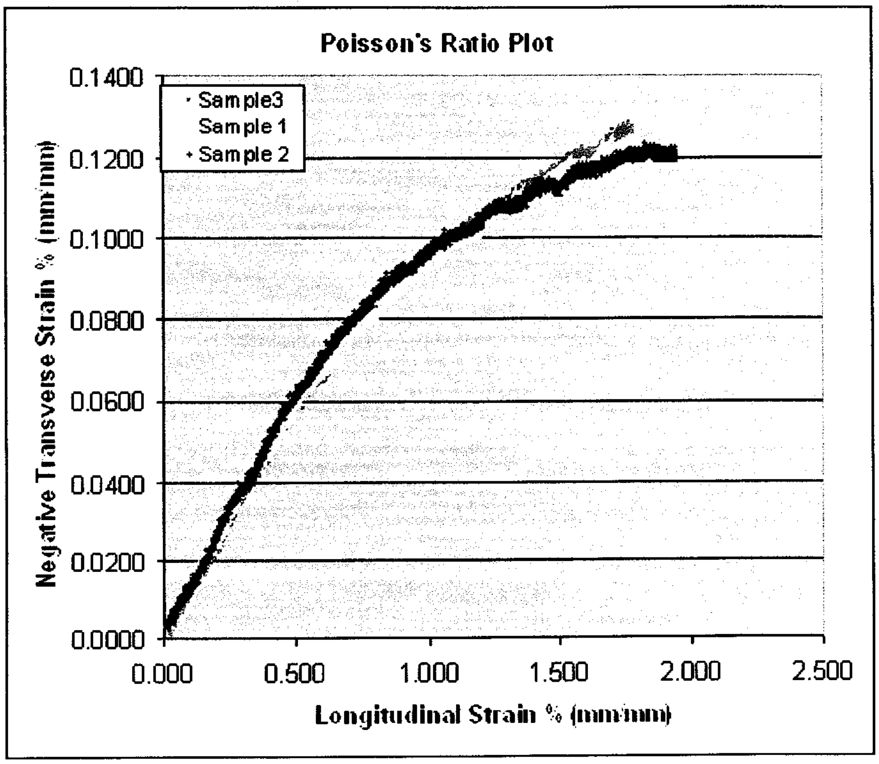

Figure 3.17 FR4 blank boards at crosshead speed of 2.44 mm/sec

The linear portion of the negative transverse strain vs. longitudinal strain plot shown in Figure 3.18 is considered to find the actual Poisson's ratio. Linear curve is fitted to find the slope. The slope found from the fitted curve Figure 3.18 gives the Poisson's ratio. The same procedure is used in all the other samples to calculate Poisson's ratio and average values from the three samples are shown in Table 3.3.

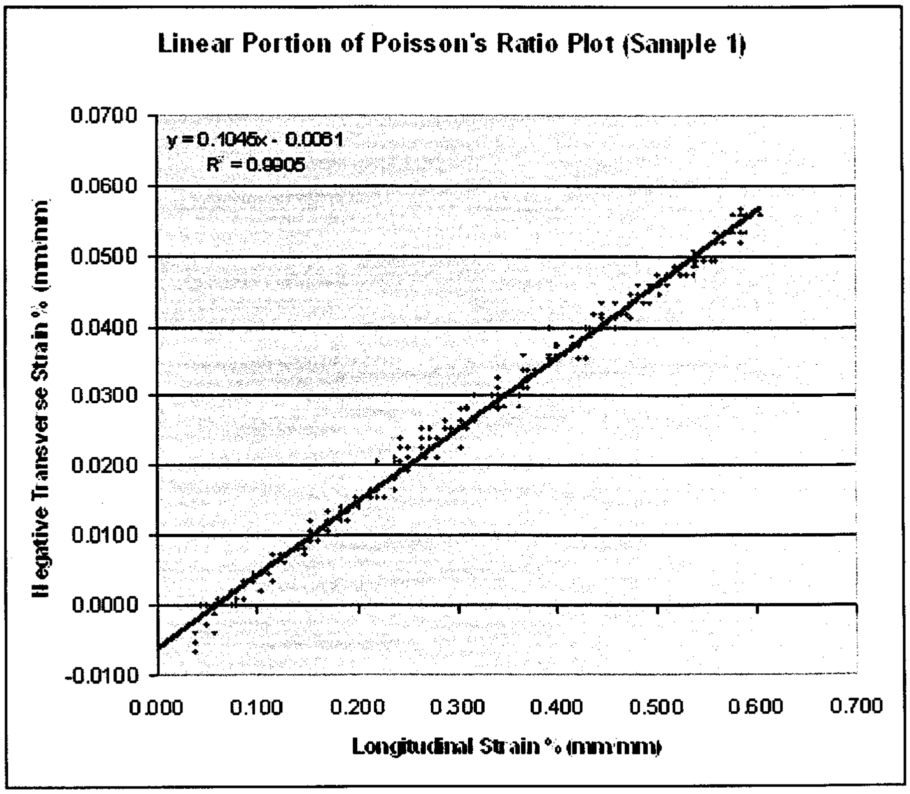

Figure 3.18 Typical results for sample 1 at crosshead speed of 0.0244 mm/sec

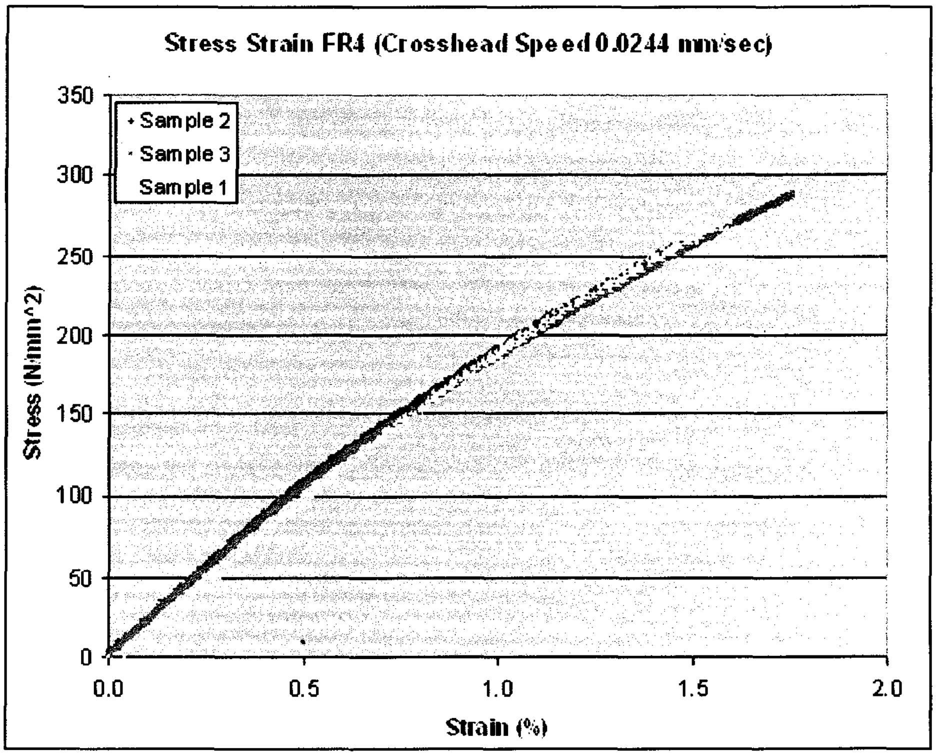

Figure 3.19 FR4 blank boards at crosshead speed of 0.0244 mm/sec

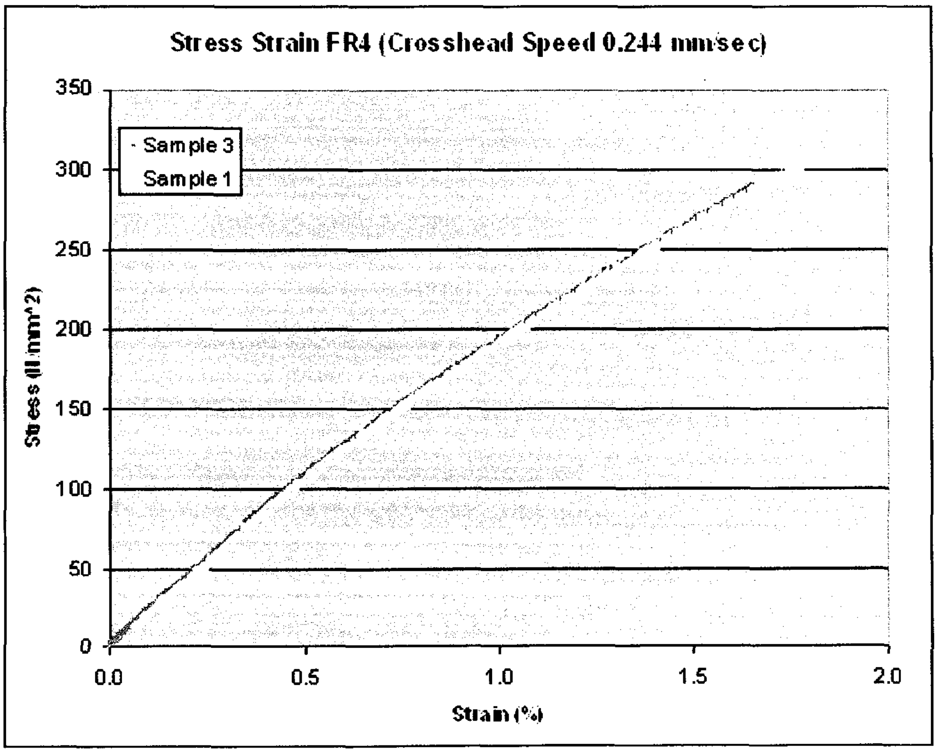

Figure 3.20 FR4 blank boards at crosshead speed of 0.244 mm/sec

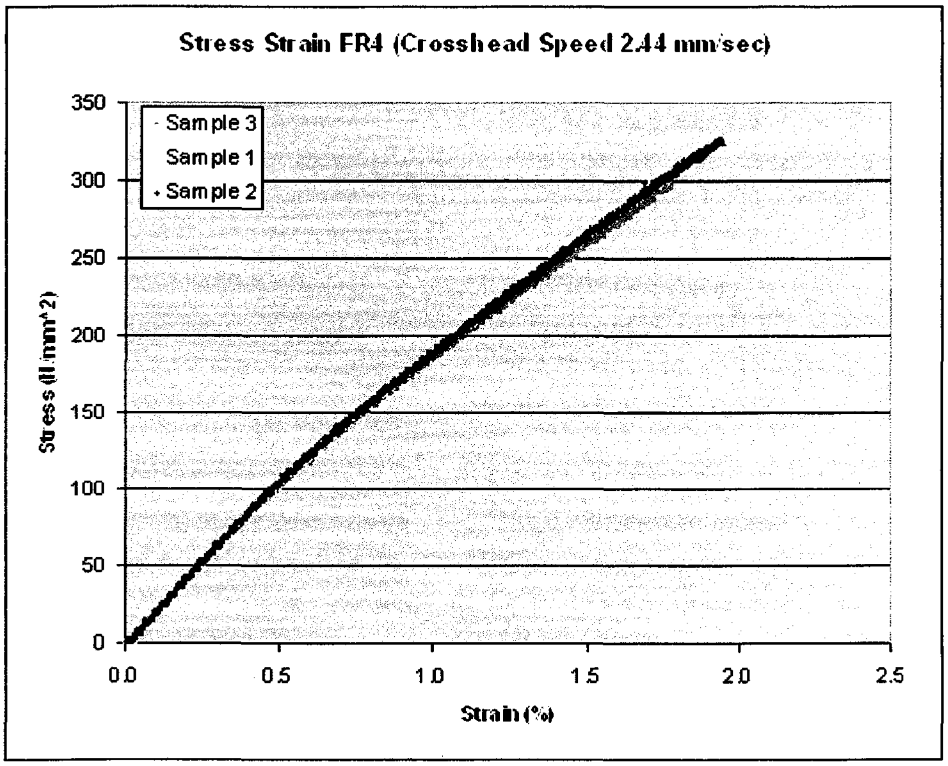

Figure 3.21 FR4 blank boards at crosshead speed 2.44 mm/sec

The linear portion of the stress vs. strain plot is considered to find the tensile modulus of elasticity. Linear curve is fitted to find the slope. The slope found from the fitted curve gives the tensile modulus of elasticity. Figure 3.22 shows one of the typical results to calculate stiffness of the material. The same procedure is used in all other samples and average values are shown in Table 3.3.

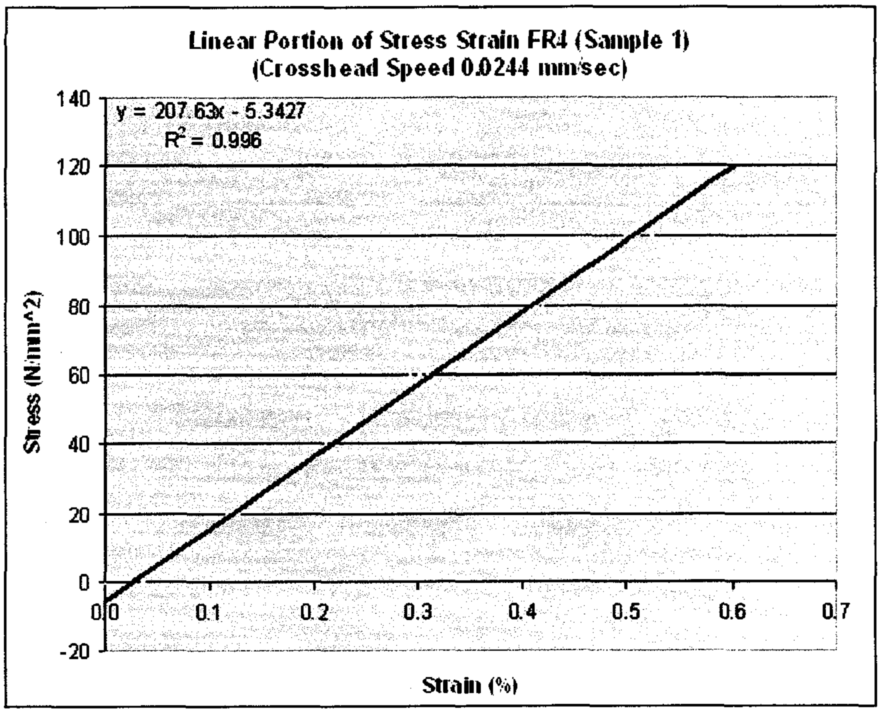

Figure 3.22 Typical results for sample 1 at crosshead speed of 0.0244 mm/sec

A linear curve is fitted to longitudinal strain vs. time plot as shown in Figure 3.23. The slope of the fitted curve yields the strain rate for sample 1. Similarly, strain rate is calculated for other samples and the average is listed in Table 3.3.

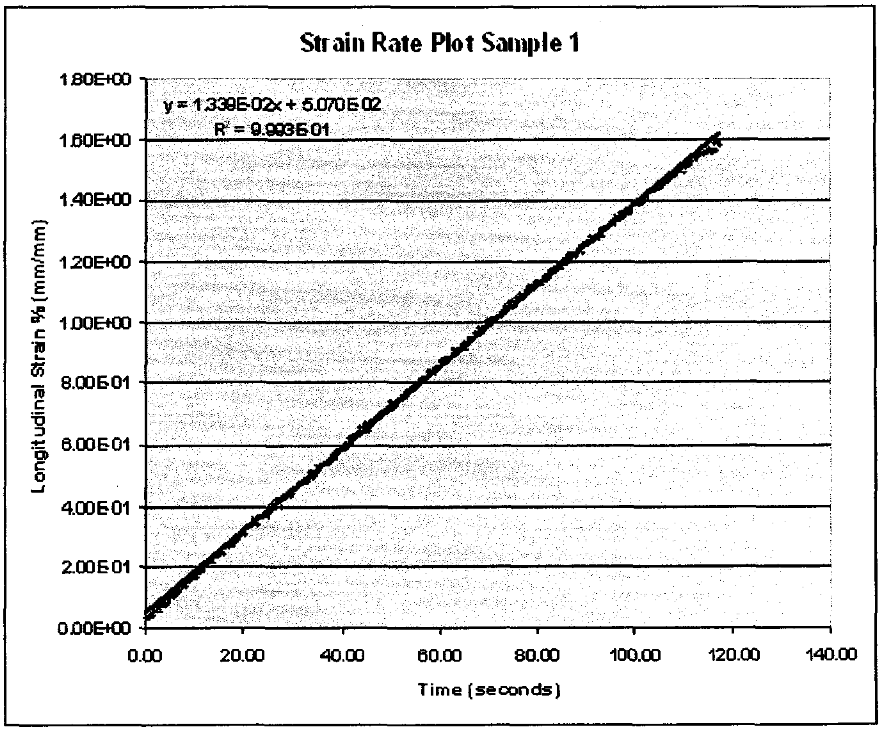

Figure 3.23 Typical results for sample 1 at crosshead speed of 0.0244 mm/sec

3.6 Results Discussion

Experimental procedures are developed for tensile testing of FR4 blank boards. Three samples are tested under each crosshead speed. The results are summarized in Table 3.3. All tested specimens exhibit consistent material properties throughout the test.

Table 3.3 Summary of Results for Tensile Testing of FR4 Blank Boards

Crosshead Speed (mm/sec)	0.0244	0.244	2.44
Poisson's Ratio	0.112	0.115	0.114
Tensile Modulus (KN/mm^2)	20.7	21.14	21.06
Strain Rate Obtained	1.34e-4	1.33e-3	1.1e-2
Tensile Strength N/mm^2	273	298.5	306.33
Failure Strain (%)	1.62	1.65	1.81

The tensile modulus and tensile strength is found to be in close accordance with related research results performed at Montana State University [36]. Failure strain and Poisson's ratio for E-glass/epoxy woven is around 0.14 and 1.9% which matches our results with [37].

CHAPTER 4

EXPERIMENTAL PROCEDURE FOR FR4 ELECTRONIC BLANK BOARDS UNDER IMPACT LOADING

4.1 Impact Testing

The term impact means applying a high value of force over a short period of time. Impact forces have greater effect than forces with lesser magnitude that is applied over a long period of time. In impact testing, an object of certain mass and velocity comes in contact with a stationary object at equilibrium which results in deceleration of the impact drop assembly by transmitting a force wave on the test specimen. This is a perfect example for imparting shock and acceleration onto an item. Mechanical shock loading occurs in many commercial and military applications. For commercial applications, shock loads may be produced by transportation, operation in vehicles, dropping an electronic assembly and during maintenance. In addition to the shock loading seen in commercial applications, military applications also have gunfire shock, missile acceleration and projectile launch shock.

4.1.1 Fixture Design for Impact Testing

The shock loads produced in the military applications can be on the order of tens of G's (acceleration of gravity) to thousands of G's. To predict failures due to shock, an experimental setup is been developed. In order to subject portion of the board to constant moment, a four-point bending approach is used. ASTM (American Society for Testing and Materials) Standard D6272 [38], is followed in performing these tests.

To achieve constant bending moment during the test, a configuration of one third span of equal lengths between the bending points is achieved as shown in Figure 4.1, 'L' is the support span and 'P' is the applied load. Sridharala S. [35] designed a similar fixture for his four-point bending experiments. It consists of three basic components: support (Figure 4.2) and impactor (Figure 4.3). Assembled view of these components in solid works is as shown in Figure 4.4. 4140 alloy steel is used as a material for all fixture components.

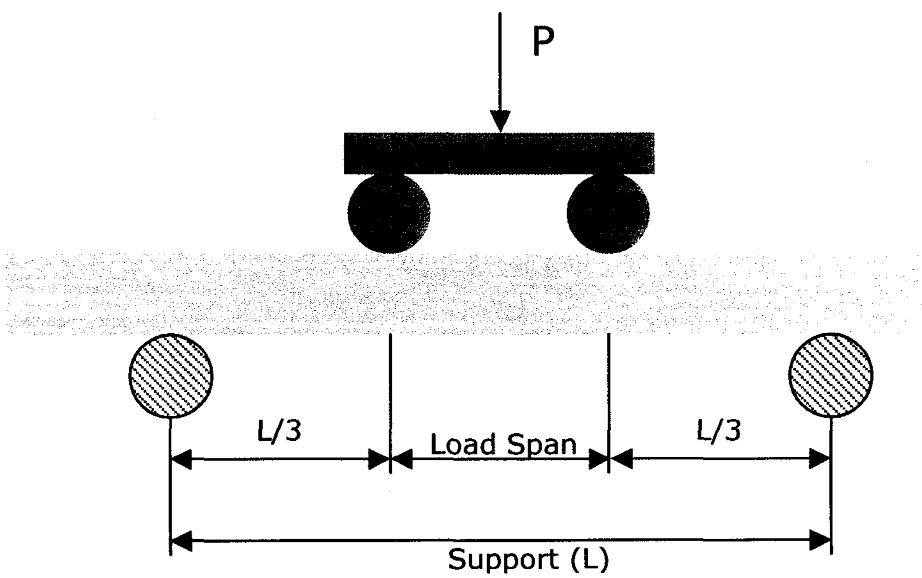

Figure 4.1: Typical four-point bending set-up

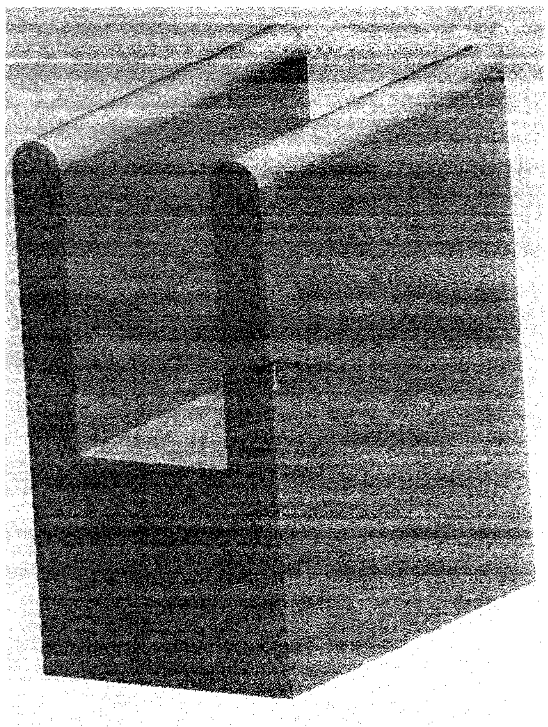

Figure 4.2: Support used for four point bending experiment

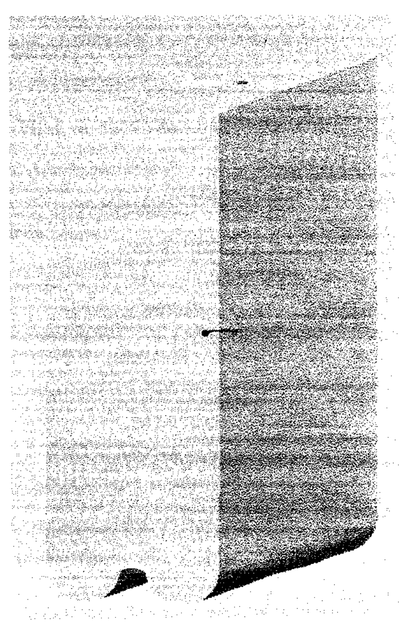

Figure 4.3: Impactor used for four point bending experiment

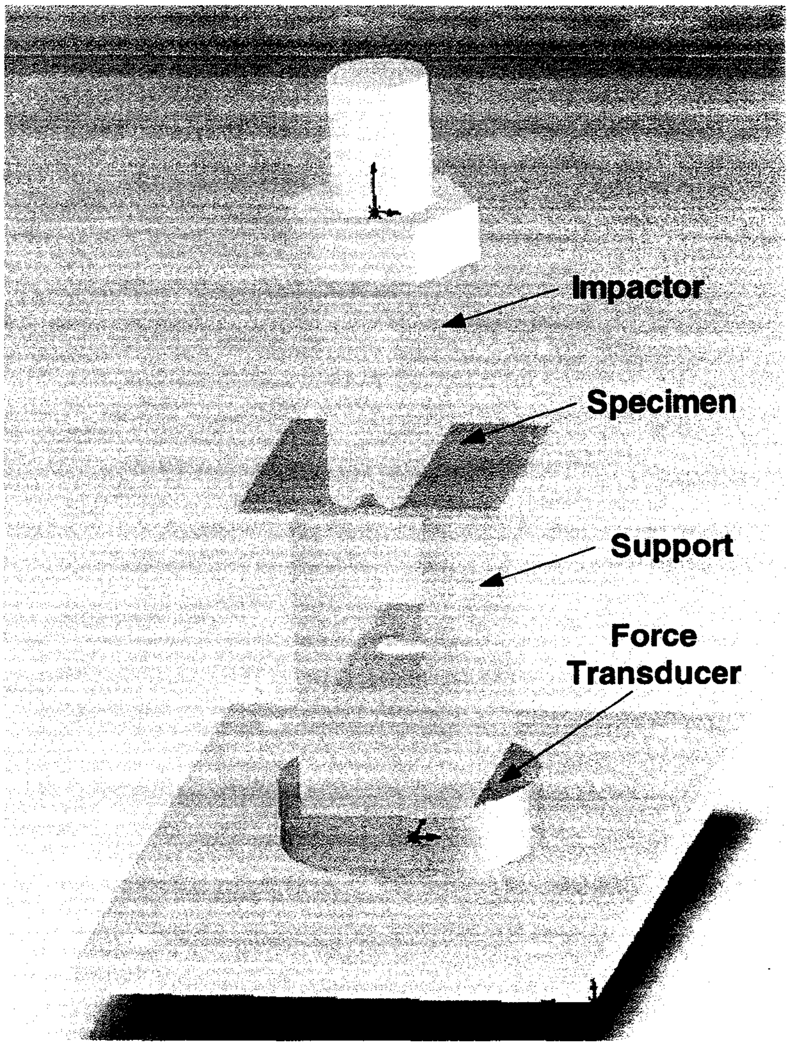

Figure 4.4: Assembled view of fixture with test specimen

Sridharala [35] conducted several four-point bending experiments at low strain rates using quasi-static and dynamic testing. To determine the strain rate dependency on the material performance of the boards, it is decided to test the boards at higher strain rates. To gain more understanding of the behavior of the boards, tensile testing is conducted to characterize the behavior of the boards under axial loading which is discussed in detail in Chapter 3.

4.1.2 Impact Testing Machine

The impact is applied on to the specimen by means of gravity load. To have the repeatable and controlled impact, Dynatup Instron 8250 drop weight impact tower is used as test equipment for performing the impact tests as shown in Figure 4.5, along with the assembly of test fixtures. Drop heights varying from 12.7 mm to 889 mm can be achieved in this machine, which can be done by adjusting the magnetic switch located behind the machine. Mass of the drop assembly may also be adjusted based on the requirement by changing the support plates in the crosshead. The stiffness of the impactor and the support are significantly higher than that of the board to reduce the possibility of interfering with the results. For this study smallest weight of 23.442 N is used at different heights as it yields the desired strain rate. Sridharala [35] used the same machine to validate his work. Procedures to operate the Dynatup Instron 8250 in gravity driven automatic mode is listed below.

1. Attach the desired weight set to the crosshead.
2. Set the control pendent switches to AUTO GRAV and, if a pneumatic clamp is installed, set the clamp ON/OFF switch to ON. When the AUTO switch is pressed, the crosshead automatically rises to the height determined by the magnetic switch. Set the pneumatic assist air pressure using the regulator on the top of the rear motor enclosure.
3. Remove any tools, other foreign objects, and the safety “H” bar from the enclosure and close the doors. The “ARM” button illuminates.
4. Press and hold the “ARM” button. The audible alarm sounds While still holding the ARM button, press the “FIRE” button. The latch hook opens allowing

the crosshead to fall and strike the specimen.

5. The latch assembly automatically retrieves the crosshead and raises it back to the height of the magnetic switch.
6. Insert safety "H" bar.
7. Remove the specimen. .

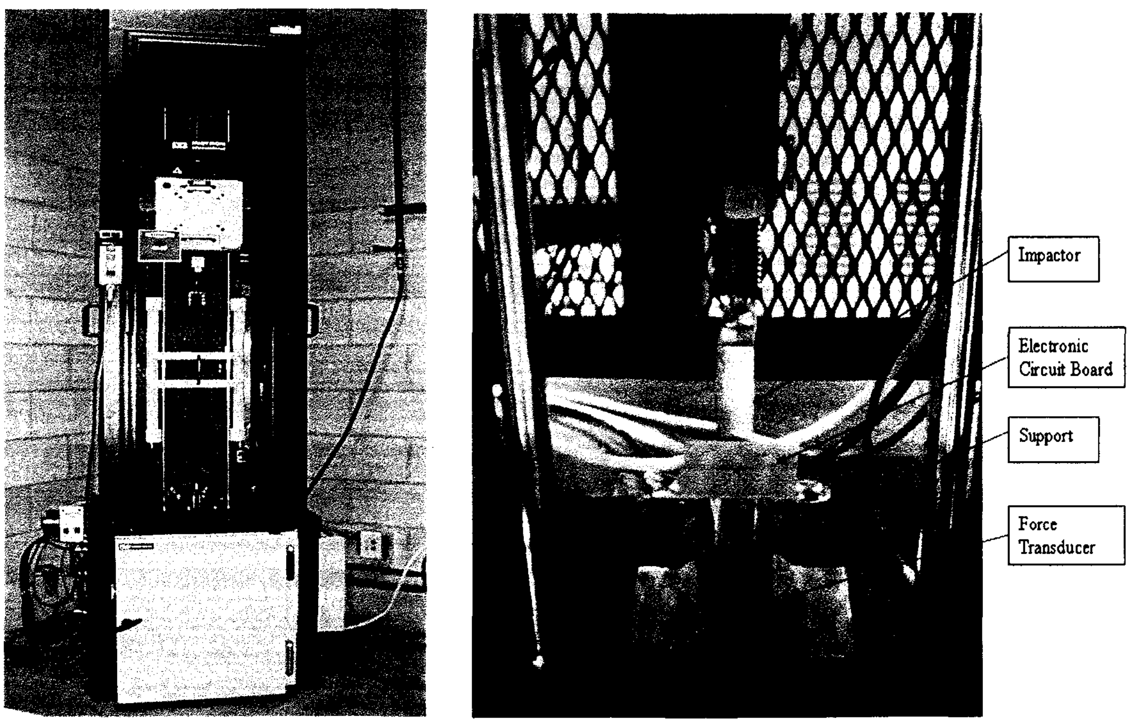

Figure 4.5: Dynatup instron 8250 drop weight impact tower and assembly of test fixtures

4.1.3 FR4 Test Specimen

The test specimen of concern is Flame Resistant 4 (FR4) which is used for making printed circuit boards (PCB). FR-4 is a material [39] from the class of epoxy resin bonded glass fabric (ERBGF). The FR4 material properties are discussed in Chapter 3. FR4 circuit boards blank (without components) with 50.8 mm by 50.8mm in dimension are used as the test specimens shown in Figure 4.6. The thickness of the board is 1.4224 mm.

4.1.4 Strain Gage Installation

Experimental analysis of structural materials sometimes requires testing to complete failure. In such cases, particularly with composite materials, failure is often preceded by large local strains, the magnitudes of which are of interest to the test engineer. Selection of proper strain gages for use in high-elongation testing is based on both anticipated strain levels and test temperature. Polyimide (E) backing is normally selected for this type of service because it has superior elongation capabilities and an operating temperature range suitable for most high-elongation testing. Properly installed and wired EA-Series [40] (polyimide-backed constantan foil) strain gages are capable of measuring maximum elongations in the range of 3% – 5%. While gage lengths of 1/8 in (3 mm) or longer will normally achieve 5% strain, shorter gage lengths may be limited to 3%. Since most structural materials (e.g., metals) yield well below this limit, the EA-Series is a popular choice for use in obtaining yield point information on these materials. For drop heights up to 76.2 mm, EA series type of strain gages is used.

As in the EA-Series, smaller gages will exhibit a lower maximum elongation capability. High elongation strain measurements place severe demands on the gage installation and necessitate special gage and adhesive selection and surface preparation procedures. EP-Series gages are recommended when measurement requirements are beyond the 3% – 5% elongation capability of the EA-Series. P-alloy is a fully annealed constantan foil processed for very high ductility. A properly bonded and wired EP-Series strain gage is capable of strain measurements to 20% (200 000 microstrain) or greater.

For drop heights varying from 152.4mm to 863.6mm, EP strain gages is used. A 350Ω resistance EP series strain gage is mounted on the central lower portion of the specimens in order to acquire the strain data shown below Figure 4.6.

The selection and implementation of proper surface preparation procedures is equally as important as using proper gages and adhesives. High-elongation measurements demand closer attention to recommended procedures than do normal elastic strain measurements. Vishay Micro-Measurements Instruction [41], surface preparation for strain Gage Bonding, outlines steps for surface preparation on a variety of materials. These procedures produce a smooth, clean surface, usually having been abraded in single direction during preparation.

High-elongation strain measurements place severe demands on the adhesive system. The adhesive must be rigid enough to prevent gage relaxation (creep), yet flexible enough to permit large deformations without cracking. Vishay Micro-Measurements [42], that outlines recommendations for gage installation and adhesive selection, gage bonding and wiring, protective coating selection for high elongation strain measurements and common installation problems.

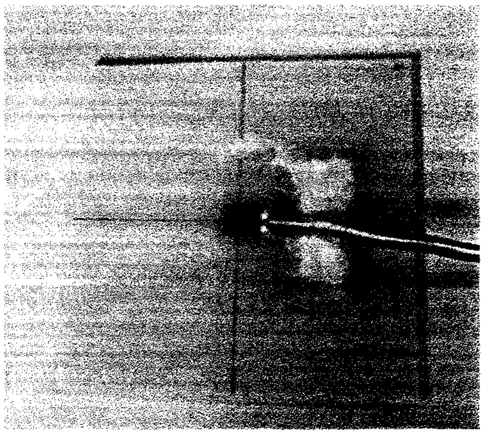

Figure 4.6: FR4 test specimen with gages

4.1.5 Data Acquisition

Data acquisition systems, as the name implies, are products and/or processes used to collect information to document or analyze some phenomenon. As technology has progressed, this type of process has been simplified and made more accurate, versatile, and reliable through electronic equipment. Equipment ranges from simple recorders to sophisticated computer systems. Data acquisition products serve as a focal point in a system, tying together a wide variety of products, such as sensors that indicate strain, flow, level, or pressure.

A PCB Piezotronics force transducer Model: 200M70 (Figure 4.7) is placed below the support portion of the fixture from which the force input is acquired by dropping the weight. Dynamic force can be measured with piezoelectric force sensors. Measurements of dynamic oscillating forces, impactor high speed compression/tension under varying conditions may require sensors with special capabilities. Fast response, ruggedness, stiffness comparable to solid steel, extended ranges and the ability to also measure quasi-static forces are standard features associated with PCB quartz force sensors. Hence quartz force sensors are recommended for dynamic force applications. They are not used as load cells for static applications.

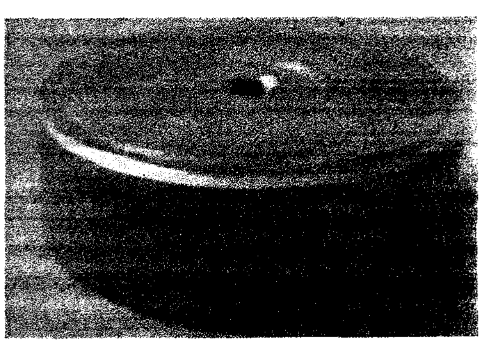

Figure 4.7: PCB piezotronics (model: 200M70) force transducer

This force transducer is connected to the PCB signal Conditioner (Model: 482A21) as shown in Figure 4.8. A signal conditioner is a device that converts one type of electronic signal into another type of signal. Its primary use is to convert a signal that may be difficult to read by conventional instrumentation into a more easily read format. In performing this conversion a number of functions may take place. For example, when a signal is amplified, the overall magnitude of the signal is increased. Converting a 0-10mV signal to a 0 -10V signal is an example of amplification.

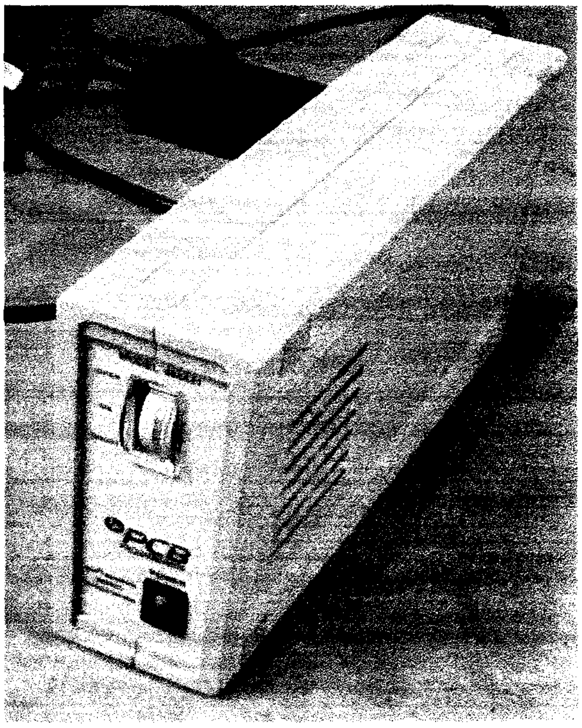

Figure 4.8: PCB signal conditioner model: 482A21

Strain gage data is acquired using a 2310A signal conditioning Amplifier. The calibration procedure for 2310A signal conditioning amplifier should be done in two stages. Each stage is discussed in detail in this section. Figure 4.9 shows the 2310A amplifier, it has four identical amplifiers. Figure 4.10 shows the layout of strain gage connection terminals to the input slot of the equipment.

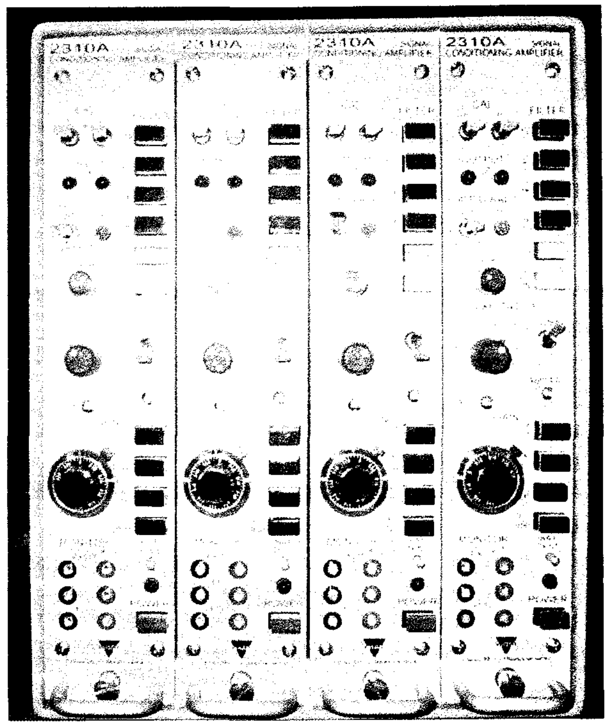

Figure 4.9: 2310 Signal conditioning amplifier

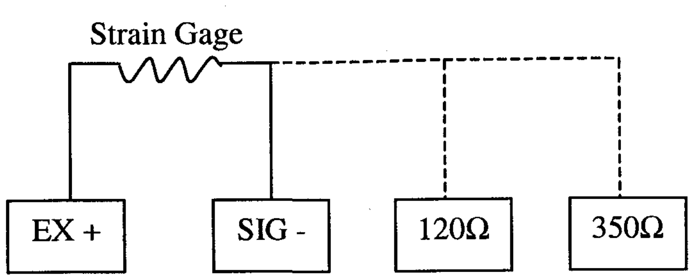

Figure 4.10: Layout of strain gage terminals to input of 2310A conditioner

Stage 1:

- For most of the dynamic/static testing, AC IN (white button) should not be depressed.
- For dynamic testing WB filter should be depressed so that it is operating in wide band equivalent to no filter.
- With a strain gage connected to the input, excitation switch still at OFF position, depress X100 gain button, both output lamps at the top of the front panel should be completely dark. If not, turn the AMP BAL adjustment below the excitation toggle switch using small screwdriver to extinguish the lamps.
- With desired bridge excitation, turn the excitation toggle switch to ON; Just below output lamps, momentarily press the AUTO BAL toggle switch all the way down to the RESET position, and release. In 1 to 3 seconds the output lamps should extinguish, indicating balance, if not repeat from AUTO BAL.
- If the lamps are still bright, turn the TRIM knob to extinguish the lamps.
- Use the following equation to determine your gain

Excitation X Gain = 2000

And set the gain according to value obtained from above equation.

By now one should see zero reading on your output monitor wherever you are displaying the signal.

Stage 2:

There are two calibration switches A and B. 'A' switch is for calibration in 200$\mu\varepsilon$ range, similarly 'B' switch is for calibration in 1000$\mu\varepsilon$ range. The following two equations relate the cal A or cal B values with the type of strain gage you are using:

$$Cal\ \mathrm{A} = \left(\frac{2}{Gagefactor}\right)200$$

$$Cal\ \mathrm{B} = \left(\frac{2}{Gagefactor}\right)1000$$

For example when using a strain gage with gage factor equal to 2, Cal A switch should be turned upwards. A 200mv signal should be read in the digital display wherever the signal is output. If it is not displaying 200mv adjust the gain so that the output will be 200mv. This calibrates the conditioner in such a way that it gives a one-to-one relation between millivolts and micro strain.

$\longrightarrow$ 1 mv = 1 $\mu\varepsilon$

With the same gain settings try turning Cal A downwards which should give -200mv, now turn cal A off and try Cal B upwards and downwards, it should read +1000mv and -1000mv respectively. If the stated voltages for corresponding switches are seen, you can turn off both Cal A & B, and can start testing. Momentarily check for the output lights, if they become bright at any time use trim knob to dim them.

The conditioning amplifier has four separate channels to amplify the data from the strain gage. It is limited to output a maximum of ±10V. In order to output voltages more than 10, the gain may be adjusted accordingly. For example, if the output voltage is 30000$\mu\varepsilon$ which is 30V (according to conversion factor discussed above). Gain can be used to reduce the output voltage by a factor of 10. Now the new output voltage is 3V. The same factor should be multiplied later to correct the reduced output voltage.

The output of the conditioner is captured using the DL 750 scopecorder oscilloscope as shown in Figure 4.11. An oscilloscope is a type of electronic test equipment that allows signal voltages to be viewed, usually as a two-dimensional graph of one or more electrical potential differences (vertical axis) plotted as a function of time or of some other voltage (horizontal axis). Sampling rate of 500Ks/s is used in all the test cases for data acquisition.

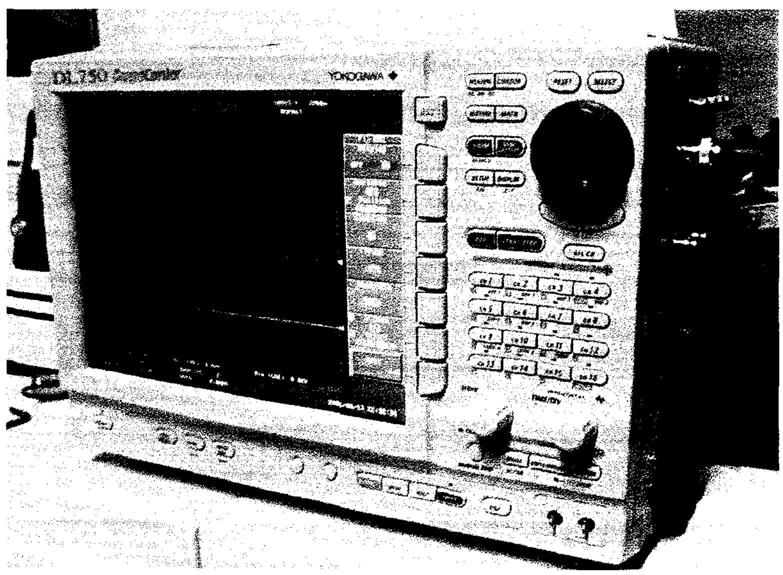

Figure 4.11 DL 750 scopecorder oscilloscope

Experimental set-up for this dynamic testing is shown in Figure 4.12. Zoomed view of the fixture and specimen along with force transducer is shown in Figure 4.13.

4.1.6 Impact Testing Results

To determine the strain rate dependency on the material performance of the boards, it is decided to test the boards at higher strain rates. Testing is conducted at various heights to obtain higher strain rates as described in Table 4.1. Three samples are tested for each drop height in order to check for the repeatability of the test. The force and strain plots obtained from three samples of each drop height are shown from Figure 4.14 through Figure 4.16.

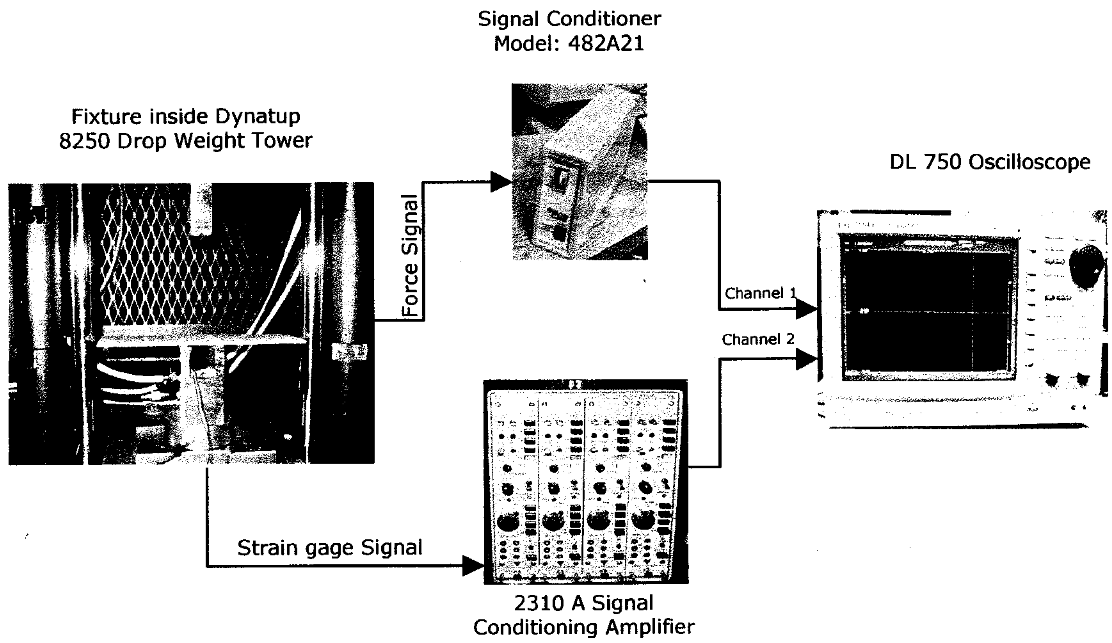

Figure 4.12 Experimental setup for dynamic testing

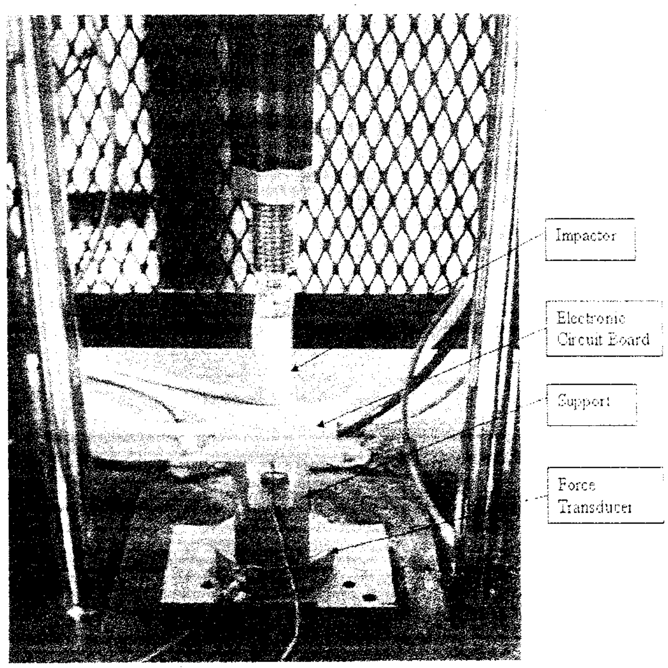

Figure 4.13 Zoomed view of the specimen, fixture, and force transducer

Table 4.1 Test matrix for 50.8mm x 50.8mm specimens

Description	Dynamic Testing		
Drop Height (mm)	76.2	152.4	863.6
Number of Blank Boards	3	3	3

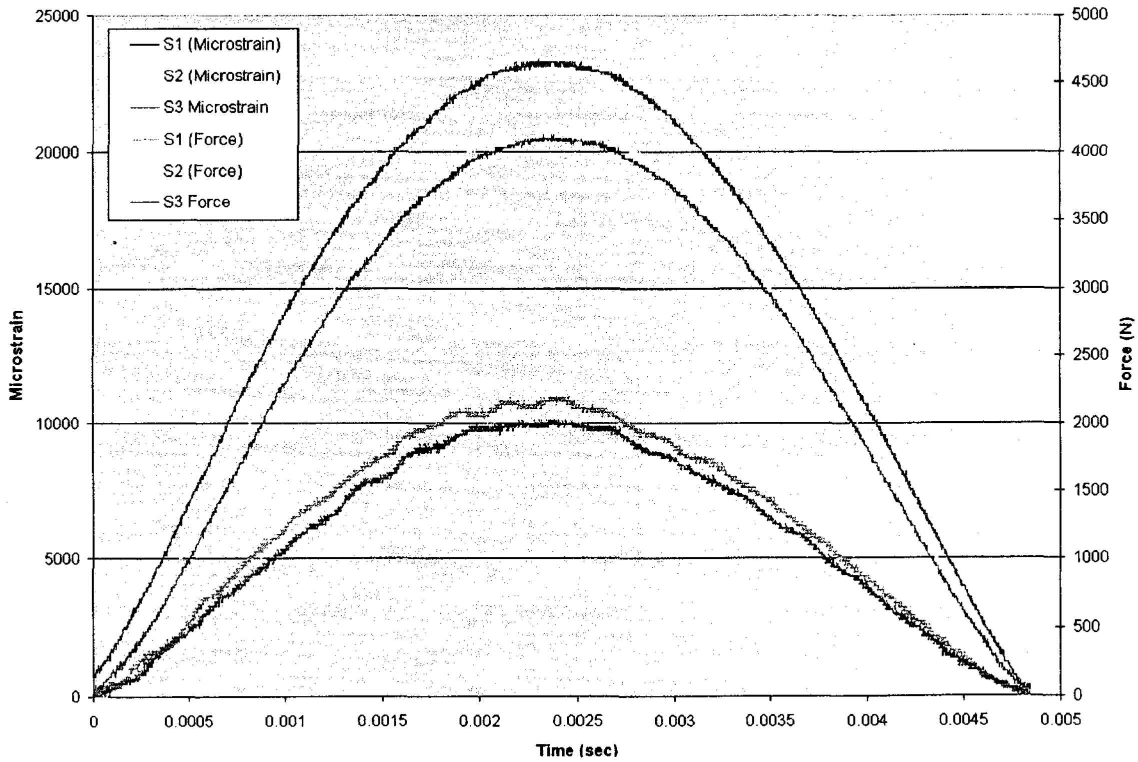

Figure 4.14 Blank boards at drop height of 76.2mm

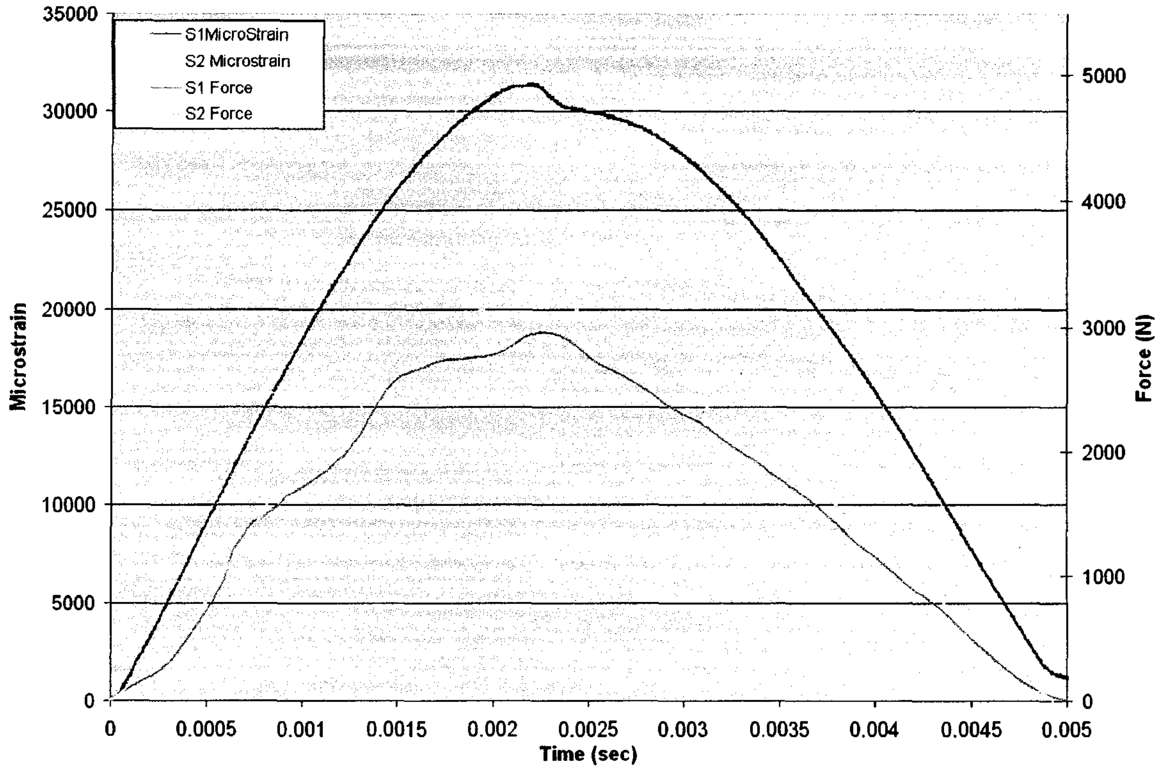

Figure 4.15 Blank Boards at Drop Height of 152.4mm

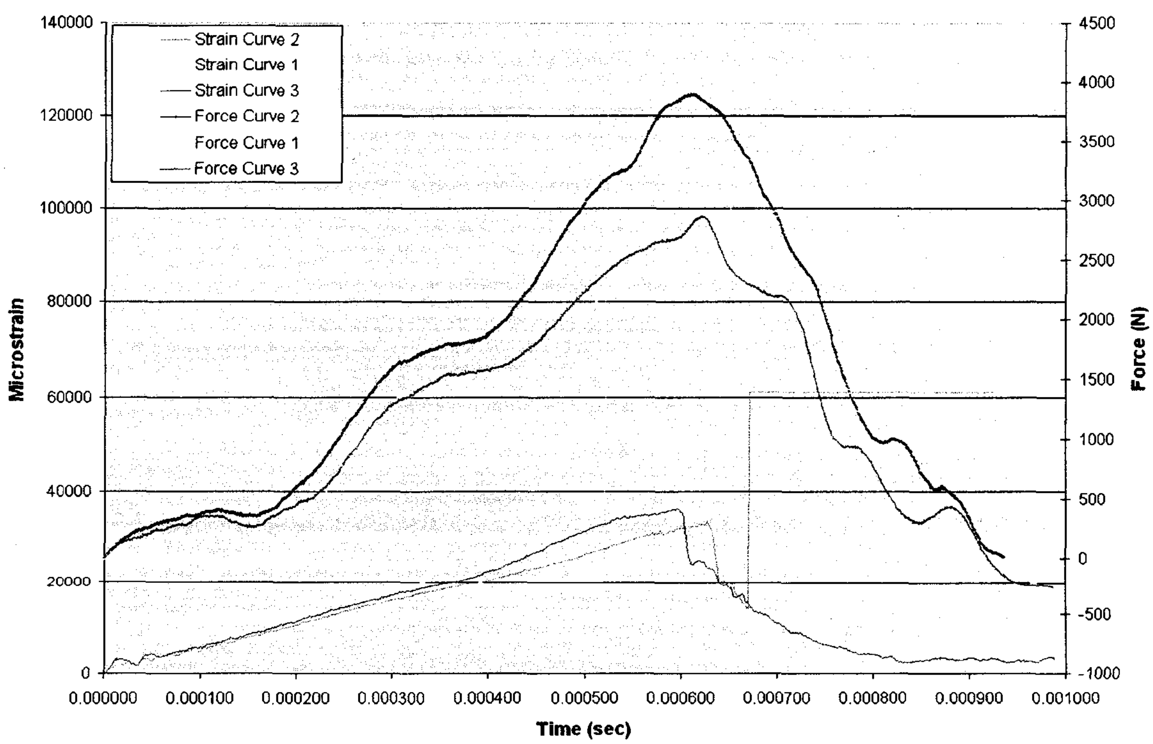

Figure 4.16 Blank Boards at Drop Height of 863.6mm

4.1.7 Discussion

Experimental procedure for shock testing of electronic circuit boards is developed. In dynamic testing, the developed experimental procedures produce repeatable results at each height. The following observations are found from experiments.

- Results show that when the impactor hits the circuit board, force and strain increase and after reaching a peak they decrease.
- As expected, peak values of force and strain increase when drop height increases.
- Test specimens failed at only 863.6mm drop height.
- For 863.6mm drop height, strain gage measures actual data up to around 0.5 milliseconds after which the gage fails. The data recorded are not considered after this time region. Reasons for gage failure could be attributed to faster deformation at higher initial velocity relatively at lesser time. The summary of results for impact testing is shown in Table 4.2.

Table 4.2: Summary of Results for impact Testing

Drop Height (mm)	50.8mm x 50.8mm Blank Boards	
	Peak Force (N)	Peak Strain (%)
12.7 [35]	800.7	0.85
26.9 [35]	1183	1.36
76.2	2188	2.33
152.4	3185	3.19
863.6	3153	3.50

CHAPTER 5

ANALYSIS OF EXPERIMENTAL DATA FROM IMPACT TESTING OF FR4 ELECTRONIC BOARDS

5.1 Introduction

Data analysis is the art of transforming data by proper evaluation and exploratory procedures to draw conclusions. Gathering data is a frequent part of solving problems and understanding the phenomenon. When we look up information to answer a question or to formulate new questions, we are gathering and analyzing data. When we conduct surveys and draw conclusions from them, we are gathering and analyzing data. This includes a lot of work with graphs and leads to mathematical tools like averaging and other computations. Depending on the type of data and the question, this might include application of statistical methods, curve fitting, selecting or discarding certain subsets based on specific criteria, or other techniques.

First step in any experiments is to begin by gathering data and analyzing by identifying attributes, sorting, and classifying objects. In our case there are two parameters to be identified and appropriate values have to be sorted to reach reasonable conclusions for them. The parameters are strain rate and flexural modulus of elasticity, which basically defines the behavior, and performance of the material to a major extent. Data analysis involving strain and force that are used in the evaluation procedures is discussed in detail in the following sections.

5.2 Data Analysis: Strain Rate Calculations

Strain values are recorded during the experiment by placing the strain gage on the bottom surface of the specimen. The deformation observed by the strain gage is measured in terms of volts. Later, the output volt is converted into microstrain by using an appropriate conversion factor as discussed in the chapter 4. Force values starting from zero and strain with positive values are considered to be the cut off point thereby avoiding the initial background noises. Since there are three samples used for each drop height, average of all these individual samples are considered for data analysis.

The impactor strikes the specimen with an initial velocity and the specimen begins to deform in bending. The specimen does not fail at the lower drop heights. Data is recorded during the loading and unloading phase of the experiment as the specimen rebounds. At 76.2mm drop height the strain rate is nearly constant during the first 1.5ms. Slope is found at this time region which yields the strain rate, Figure 5.1. There is a small initial nonlinear region when the loading starts. The impactor slows to zero velocity at about 2.3ms. The strain rate is very non-linear from 1.5ms-3.5ms when the specimen slows to stop and then gradually begins to rebound. The strain rate is nearly constant again during the final unloading phase. The average initial strain rate during the loading phase is equal to the slope of the fitted straight line as shown in Figure 5.1 in red color. Strain rates for loading and unloading phases are listed in Table 5.1. It is found that unloading strain rate is slightly slower because some energy is lost due to friction, specimen heating and possibly internal damage.

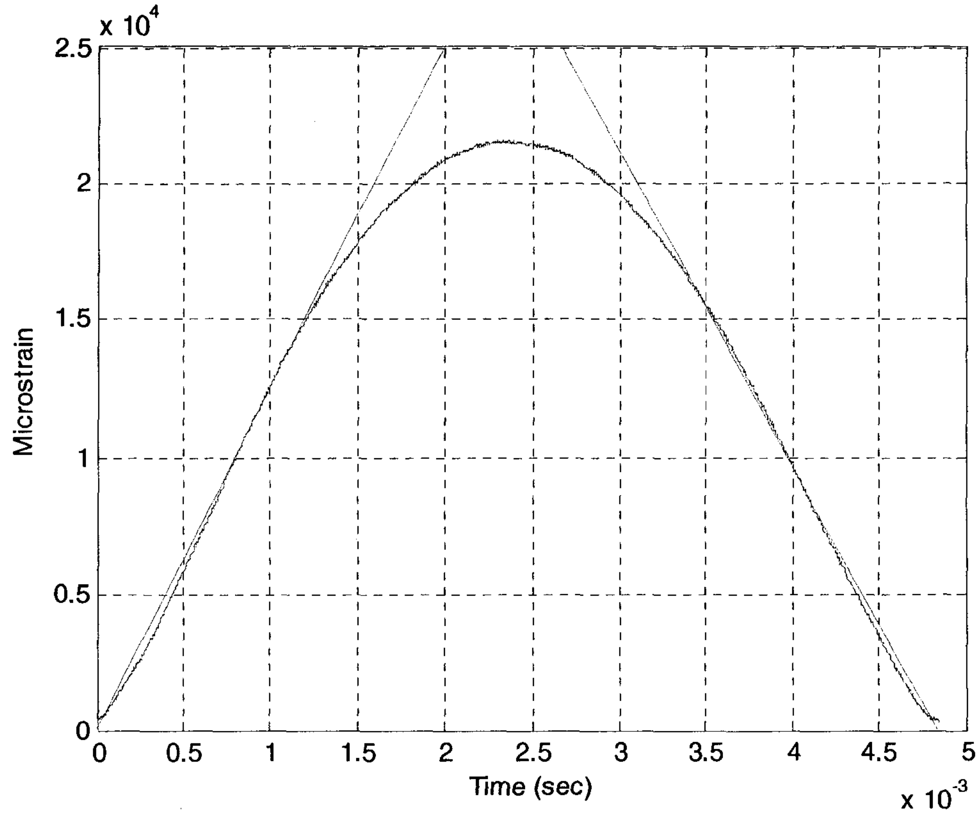

Figure 5.1: Fitted microstrain at 76.2mm drop height

The test data for the 152.4mm drop height (Figure 5.2) shows similar trends but higher strains are reached because of higher impact energy. Fitted straight line is used to calculate strain rate is shown in red color in Figure 5.2. Some internal damage is obtained in the specimens tested at this height after the experiment, as shown in Figure 5.3. A small kink in the experimental strain is observed at the peak levels, which may be due to specimen cracking. Strain rates for loading and unloading phases are listed in Table 5.1 The strain rate during unloading changes more in this case because there is more internal damage in the specimen.

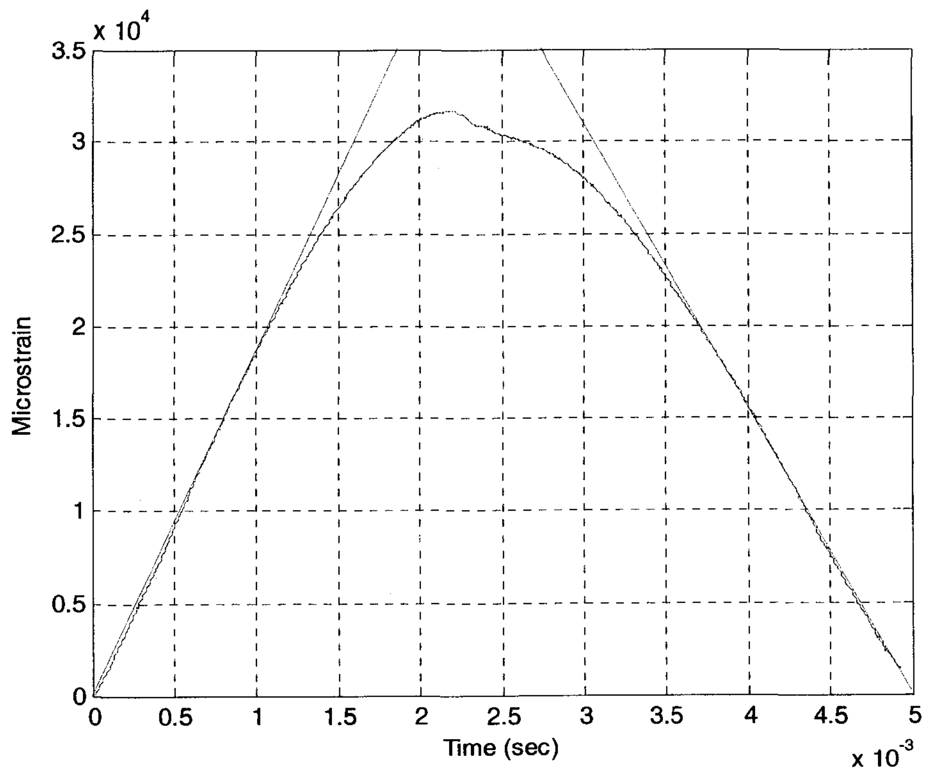

Figure 5.2: Fitted microstrain at 152.4mm drop height

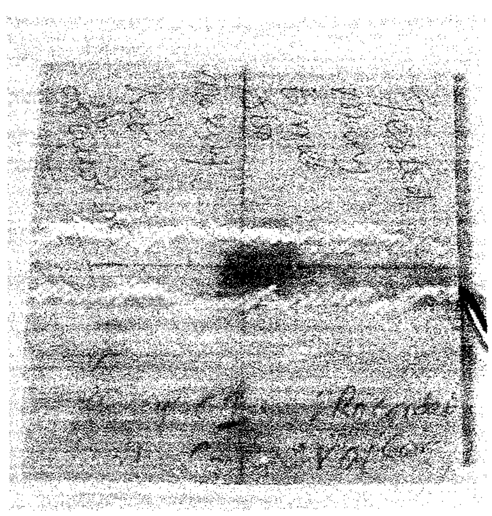

Figure 5.3: Specimen showing internal damage tested at 152.4mm drop height.

The strain data for the largest drop height is different when compared to smaller drop heights. These specimens are loaded to failure so there is only loading portion as shown in Figure 5.4. The curve is almost linear. There is an initial phase up to 0.3ms where the strain rate is nearly constant. Then there is a slight shift in the curve and the strain rate appears to increase slightly. There is possibly some initial failure which reduces the laminate stiffness causing the strain rate to increase. The fitted straight line to calculate strain rate is shown in red color in Figure 5.4. The overall average strain rate is listed in Table 5.1.

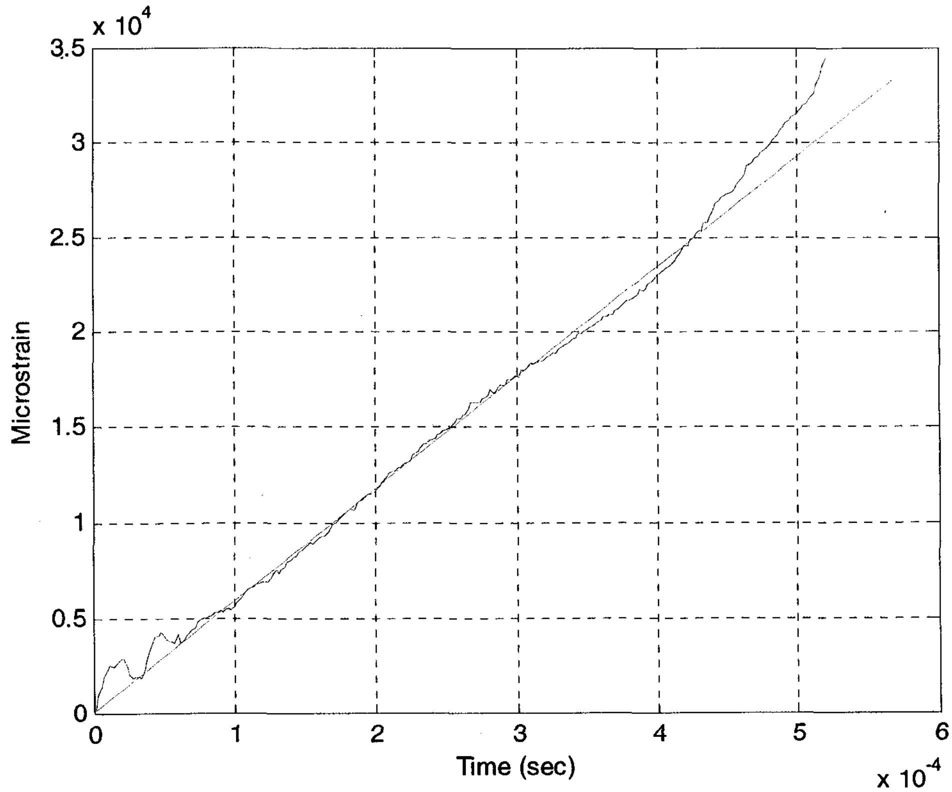

Figure 5.4: Fitted microstrain at 863.6mm drop height

5.3 Data Analysis: Flexural Modulus of Elasticity Calculations

Flexural modulus of elasticity for four point bending is calculated using simple beam theory. Figure 5.5 shows the four point setup with supporting fixture, crosshead and the board.

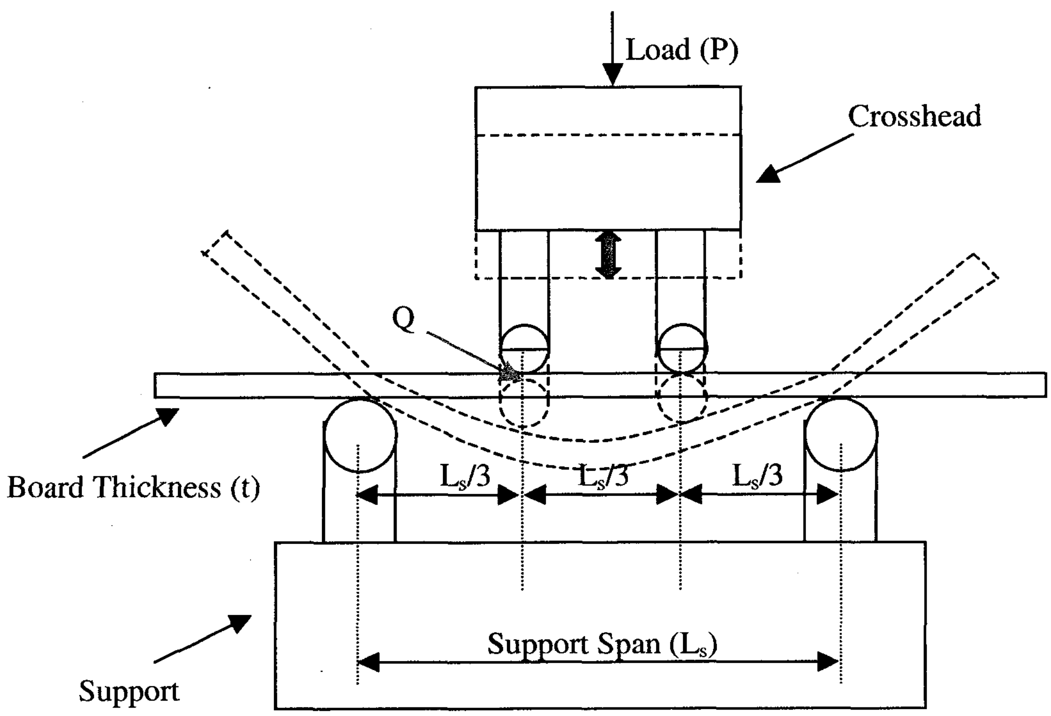

Figure 5.5: Four point bending setup

The cross head or the impact drop assembly transmits the force due to gravity on to the specimen. The deflection of the board is modeled as simply supported beam as shown in Figure 5.6.

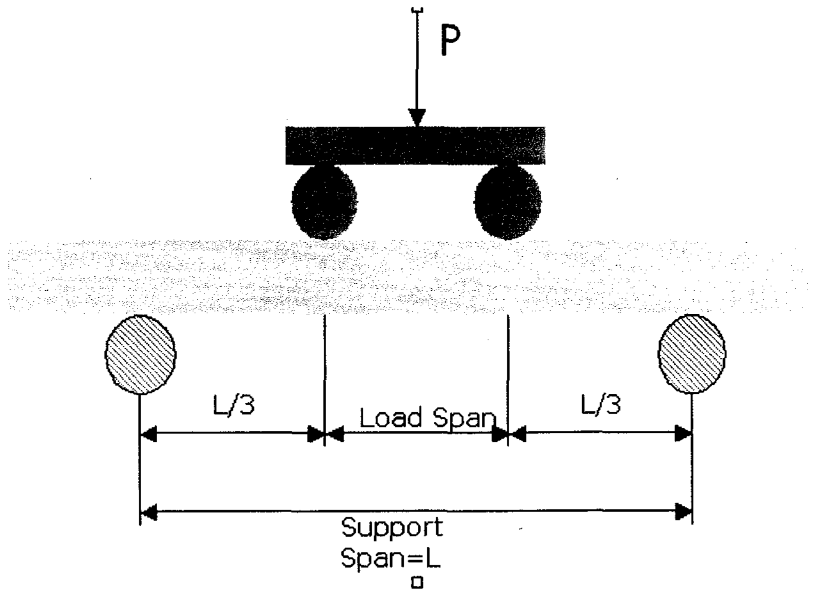

Figure 5.6: Equivalent simply support beam

The bending moment equation for the middle section of the board (Ignoring the Poisson's ratio effect of a board in bending) is given by,

$$\sigma = \frac{\left(\frac{P}{2}\right)\left(\frac{L}{3}\right)\frac{h}{2}}{\frac{bh^3}{12}} = \frac{PL}{bh^2} \qquad (1)$$

where, P is the applied load,

L is the length of the board between supports,

h is the thickness of the board, and

b is the depth of the board.

The bending stress is calculated from equation 1. Stress strain curves are plotted for each drop height to find the slope using a straight fitted line, which yields the flexural modulus of elasticity as shown in Figure 5.7 through Figure 5.9. The stress strain curves for 76.2mm and 152.4mm drop height (Figure 5.7 and Figure 5.8) has two phases:

loading and unloading phase of the impactor as indicated by the arrows. Variation in strain rate causes the stress strain curve to separate at 152.4mm drop height as shown in Figure 5.8. For the higher drop height of 863.6mm (Figure 5.9) there is only loading phase as explained in Section 5.2.

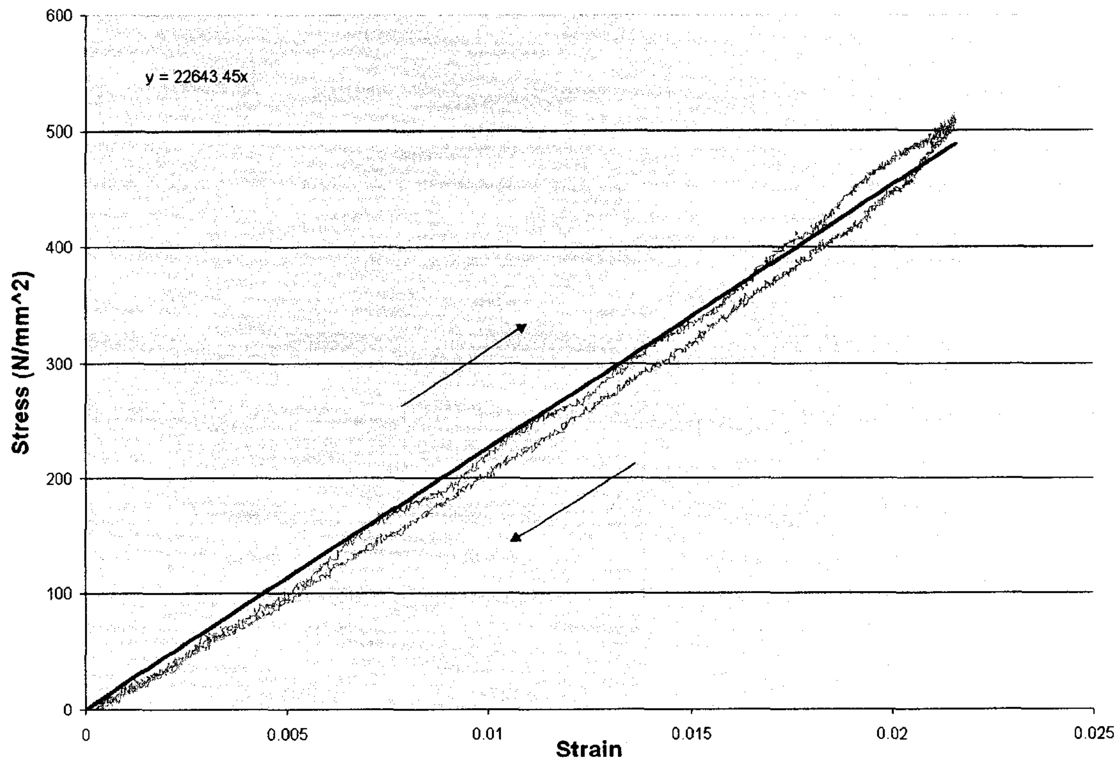

Figure 5.7: Stress strain curve for 76.2mm drop height

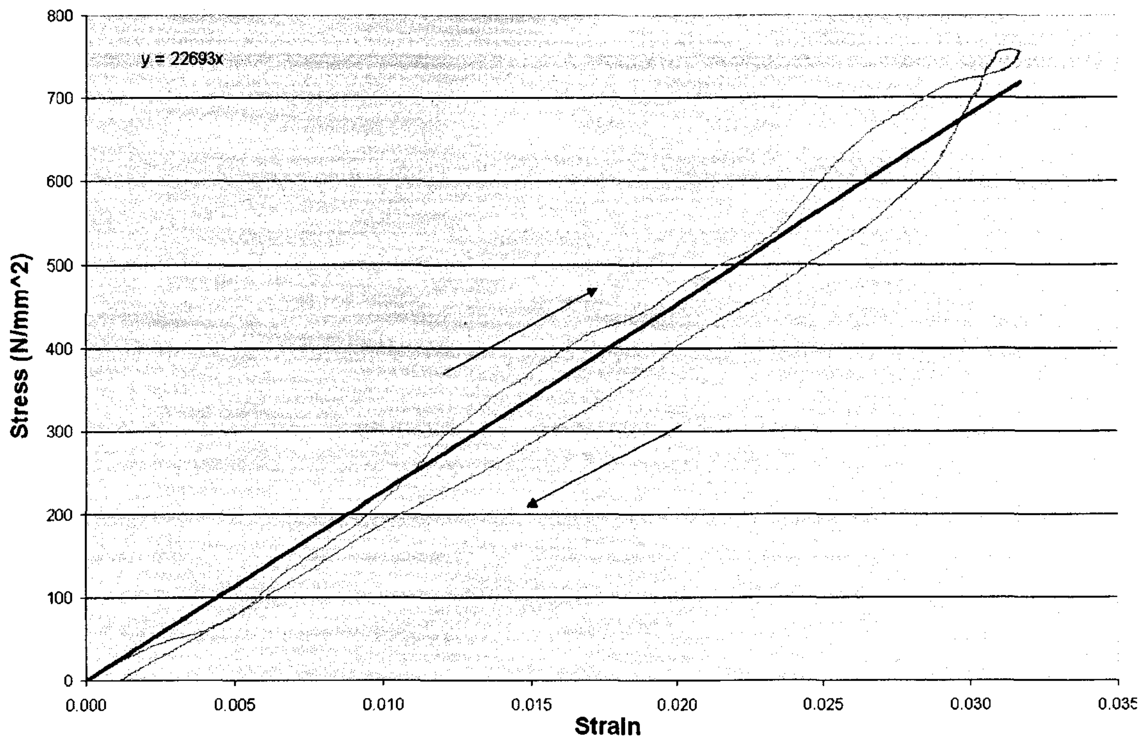

Figure 5.8: Stress strain curve for 152.4mm drop height

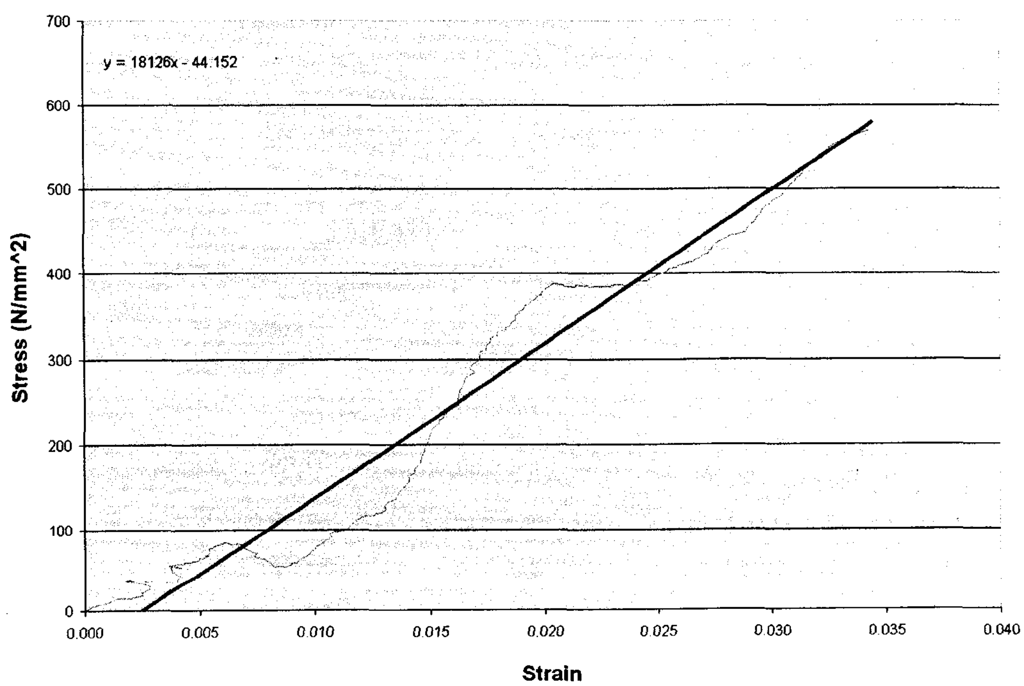

Figure 5.9: Stress strain curve for 863.6 drop height

Sridharala [35] performed dynamic four point bending experiments on the same material. His results are also shown in Table 5.1 for the purpose of comparing the flexural modulus with respect to higher strain rate. A plot comprising of tensile and flexural modulus vs. strain rate is shown in Figure 5.10. The strain rate is plotted in logarithmic scale for the purpose of showing all ranges of strain rate clearly. Modulus of the test material is found to be constant for most of the tested strain rate.

Table 5.1: Results for impact testing

Drop Heights (mm)	Peak Force (N)	Peak Strain (%)	Average Strain Rate (mm/mm/s)		Average Flexural Modulus of Elasticity (KN/mm^2)
			Loading Phase	Unloading Phase	
12.70 [35]	800	0.85	4.32	-4.31	22.57
26.92 [35]	1183	1.36	7.31	-6.97	20.71
76.2	2189	2.33	12.48	-12.03	22.64
152.4	3140	3.19	18.4	-15.5	22.69
863.6	3154	3.50	60.2	-	18.12

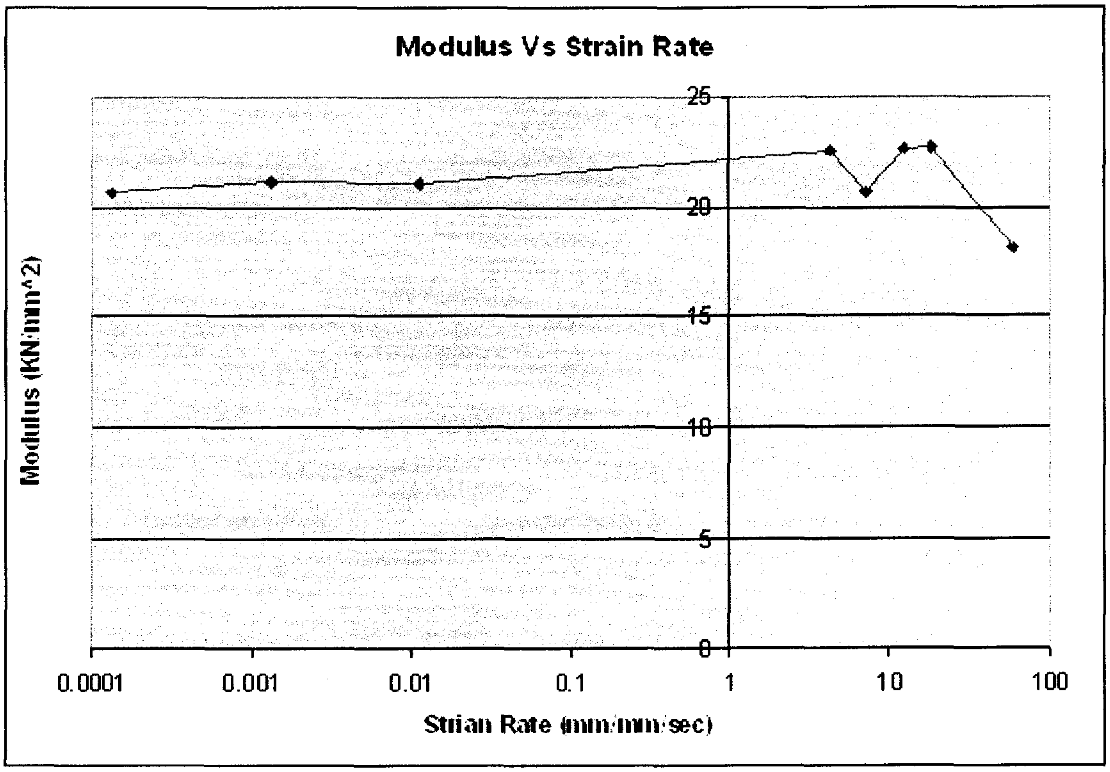

Figure 5.10: Modulus vs. strain rate for all samples tested

Stress strain curves obtained under uniaxial tensile testing, quasi-static four point bending and dynamic four point bending are compared as shown in Figure 5.11. Four point bending and tensile testing stress strain curves reasonably match during the initial period. Further research is needed to test more samples under higher strain rates to understand the behavior of these stress-strain curves for the comparative study.

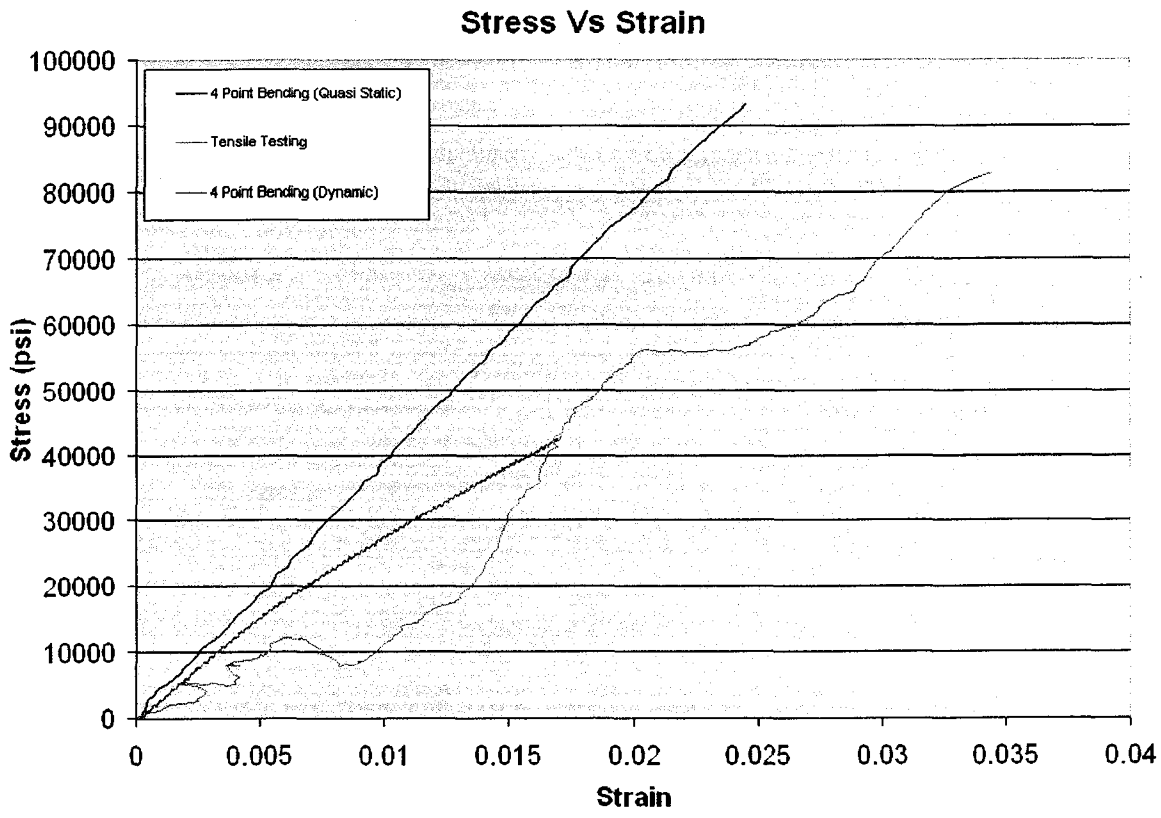

Figure 5.11: Stress vs. strain for all experimental cases

CHAPTER 6

FINITE ELEMENT ANALYSIS OF SHOCK/IMPACT TESTING

6.1 Objective

FEA is performed to simulate the experimental situation and study the material behavior under impact loading. FEA for the test cases are modeled in order to compare them with the experimental results. FEA setup has three basic components, impactor, electronic board and support, similar to experimental fixture. The FEA results are used to identify appropriate material models and element types that can be used to model these situations accurately. In order to study the Young's Modulus dependency on strain rate, the simulation is done for all the three drop heights used in the experiments.

6.2 System and Software

All the computational analysis is done on a 3 GHz Intel Zeon dual core processor, having a 3 GB RAM. Altair HyperMesh v7.0 [44] is used as the pre-processor to create and mesh the 3D models of impact testing setup. Explicit FE code LS-DYNA v970 [45] is used to simulate the structural response of the FE models. LS-POST and Altair Hyper View v7.0 are used for post-processing the analysis.

6.3 Element Types

Two basic types of elements are used in meshing the FEA impact test setup. The impactor and support are meshed with solid brick elements while the electronic board is meshed with shell elements.

6.3.1 Shell Element

The shell elements used in the FE model are 4-noded with bending capabilities. Both in-plane and normal loads are permitted. The element have twelve degrees of freedom at each node: translations, accelerations and velocities in the nodal x, y and z directions and rotations about the x, y and z axes as shown in Figure 6.1. This type of element is used in explicit dynamic analysis [46].

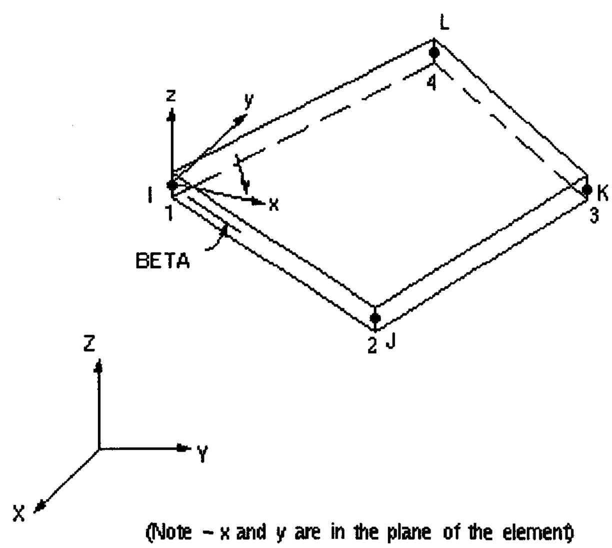

Figure 6.1: Scheme of a shell element [46]

The Belytschko-Lin-Tsay shell type of element formulation is used for this shell element. This is the default shell element formulation used in LS-DYNA due to its computational efficiency. The Belytschko-Lin-Tsay shell element [46] is based on a combined co-rotational and velocity strain formulation. The efficiency of the element is obtained from the mathematical simplifications that result from these two kinematical assumptions. The co-rotational portion of the formulation avoids the complexities of nonlinear mechanics by embedding a coordinate system in the element. The choice of velocity strain, or rate deformation, in the formulation facilitates the constitutive evaluation.

6.3.2 Solid Element

Solid element is used in meshing the impactor and support. This type of element consists of eight nodes as shown in Figure 6.2.. These elements have nine degrees of freedom at each node: translations, accelerations and velocities in the nodal x, y and z directions and rotations about the x, y and z axes. This type of element is used in explicit dynamic analysis [46].

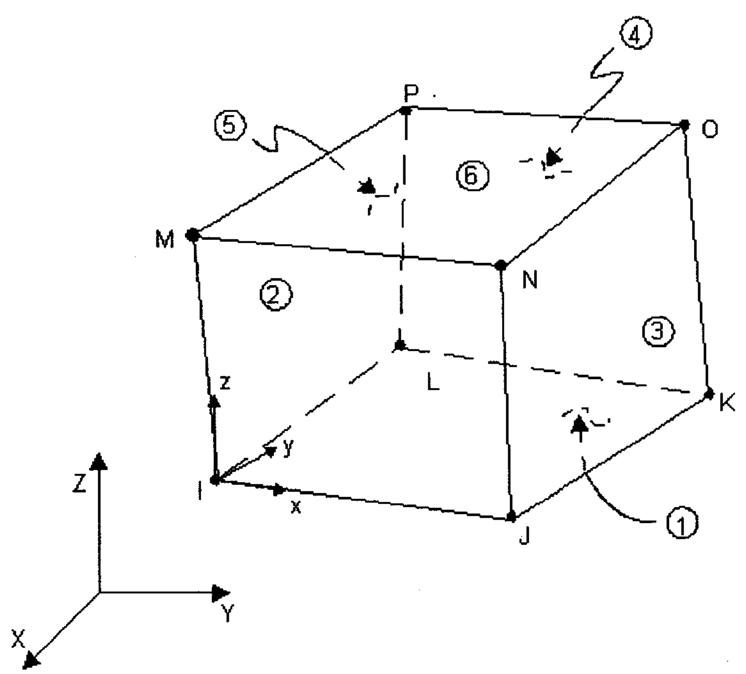

Figure 6.2: Scheme of a solid element [46]

The geometry, node locations, and the coordinate system for this element are shown in Figure 6.2. By default this element uses reduced (one point) integration for faster element formulation.

6.4 Model Creation and Meshing

FEA model is created and meshed in Altair HyperMesh. Initially temporary nodes are created in HyperMesh. Two dimensional surfaces are drawn for impactor and support using these nodes, shown in Figure 6.3. Temporary nodes are joined by lines and arcs option, in the *geom* menu of HyperMesh, to form the skeleton for impactor and support. Impactor and support is extruded by using the drag option in the *2D* menu of HyperMesh as shown in Figure 6.4. In the 2D direction, the model is meshed with hundred and fourteen elements and along the drag direction there are forty-eight elements present.

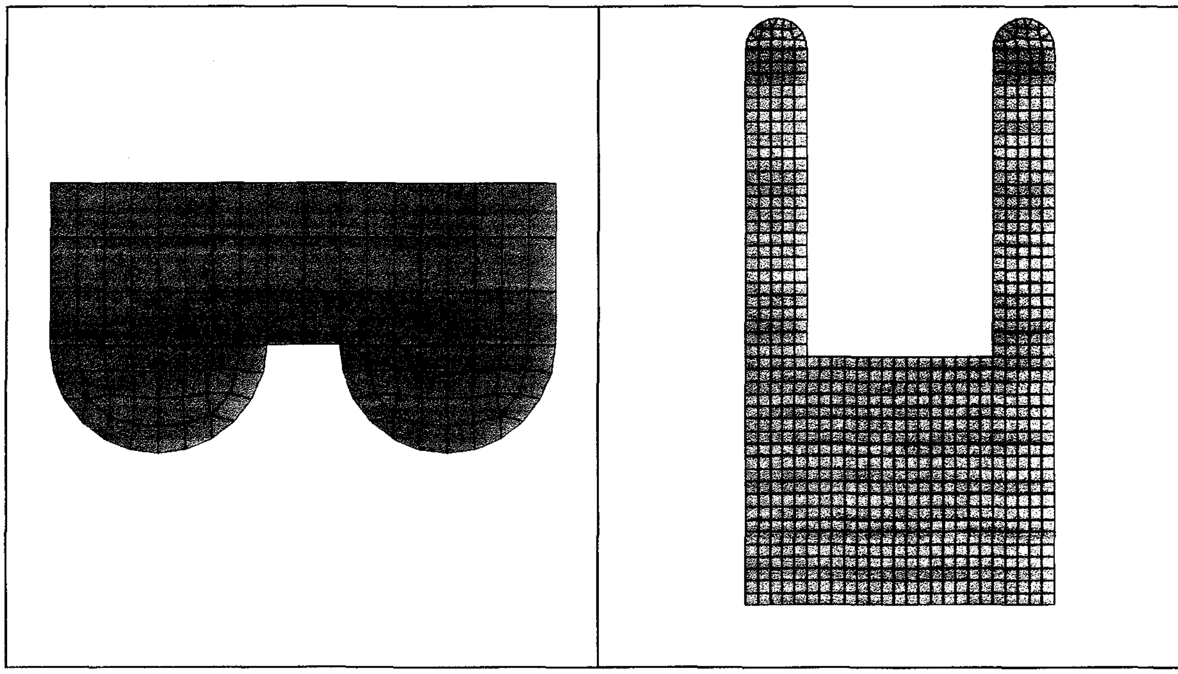

Figure 6.3: Two dimensional mesh of impactor and support.

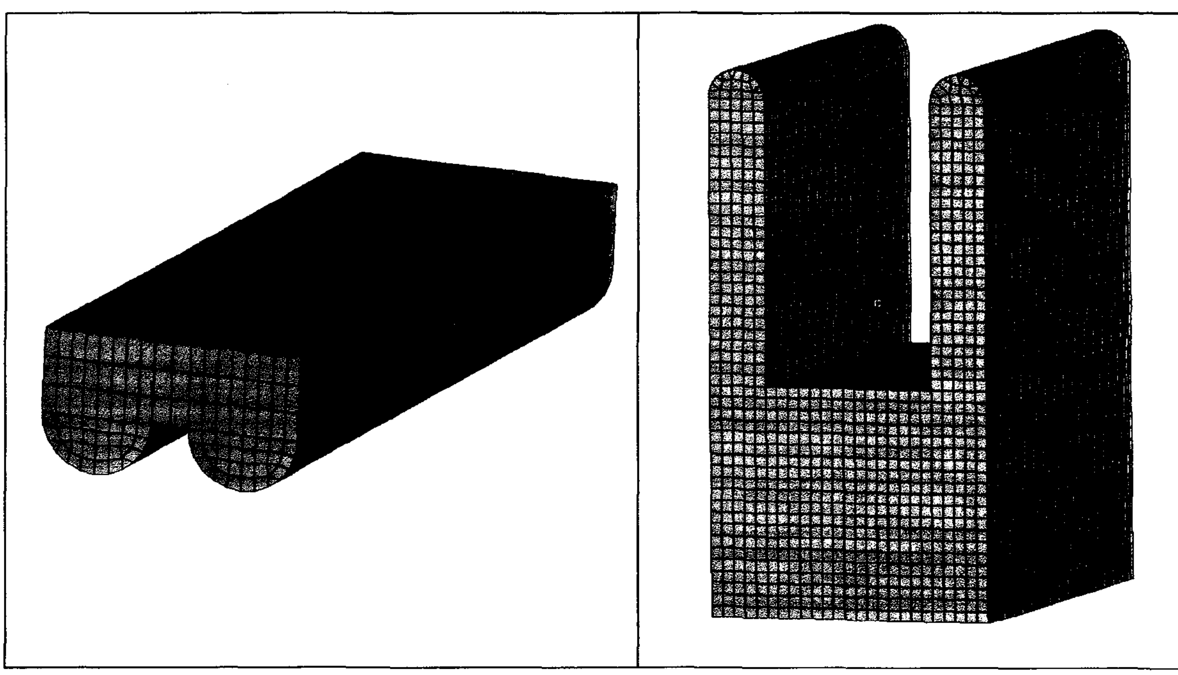

Figure 6.4: Three dimensional mesh of impactor and support.

Electronic board is meshed using 64 by 48 shell elements. A larger number of elements are created in the longitudinal direction to better model bending of the board. Meshed model of the board is shown in Figure 6.5. Figure 6.6 shows the complete meshed model of the impact testing setup, which has the same dimension as that of the experimental setup, except the height of the impactor is reduced to decrease the number of elements thereby, decreasing the FEA computational time.

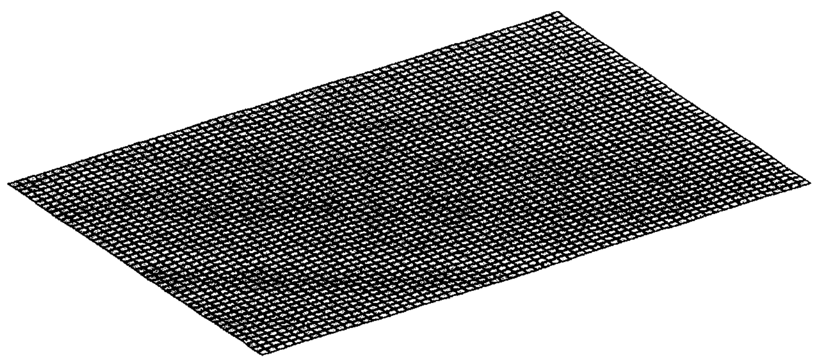

Figure 6.5: Meshed model of the circuit board

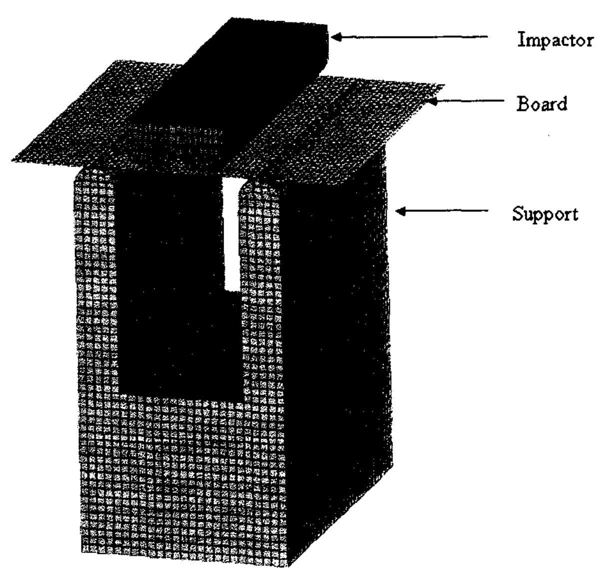

Figure 6.6: Meshed model of impact testing setup

6.5 LS-DYNA Input Cards

An input file is created in LS-DYNA after modeling the whole setup. In LS-DYNA all the information about the model is written in the form of cards in the input file. Cards are the commands, which contain information about various aspects of the model such as node and element definitions, materials, loads, boundary conditions etc. The following cards are used in the current model.

1. Control cards
2. Database cards
3. Material cards
4. Cards defining the parts and sections
5. Cards defining the nodes, elements
6. Contact cards
7. Cards defining the boundary conditions
8. Cards defining the loads
9. Cards defining box
10. Cards defining output

Detailed descriptions of some of these cards are explained later in this chapter and others cards referred to LS-DYNA [45].

6.6 Material Characteristics

In the FE models two types of material models are defined. The type and properties of these materials can be defined in the MAT cards available in LS-DYNA. Material type

MAT1 is used to define the steel properties for the impactor and support. MAT2 is used to represent the material model for the electronic board.

6.6.1 MAT1

MAT1 card is named as *MAT_ ELASTIC in the LS-DYNA input file. This material model is used to define the elastic-isotropic behavior of beam, shell and solid elements. Below is a sample of MAT1 card used in the electronic boards.

```
 *MAT_ELASTIC

$HMNAME MATS        3 Impactor & Support
$---------1---------2---------3---------4---------5---------6---------7
        MID       RO         E        PR
          37.8500E-06      210       0.3
```

where,

- MID defines the material identification number. This number is used to assign this material to the parts in the model. (Definition is mandatory).
- RO defines the mass density. (Definition is mandatory).
- E defines the Young's modulus. (Definition is mandatory).

6.6.2 MAT2

MAT2 card is named as *MAT_ORTOTROPIC_ELASTIC in the LS-DYNA input file. This material model is used to define the elastic-orthotropic behavior of the composite layers. Since the electronic board is an orthotropic material, it is required to define the properties in three mutually perpendicular directions shown in Figure 6.7. The thickness of the orthotropic material is very small and hence plane-stress condition is assumed for these materials. Therefore the properties in the thickness direction (c) are assumed to be greater than or equal to those along (a) and across (b) the fibers for the composite.

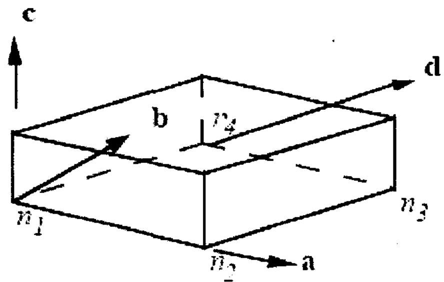

Figure 6.7: Element having orthotropic material property [45]

This card can be used for models with solid or shell elements that are orthotropic in nature. Below is a sample of MAT2 card used in the electronic boards.

```
  *MAT_ORTHOTROPIC_ELASTIC
$HMNAME MATS          2Board
$        MID          RO         EA         EB         EC       PRBA       PRCA
$---------1---------2---------3---------4---------5---------6---------7
           21.7300E-07      21926      21926     9101.4       0.12       0.18

$       PRCB        GAB        GBC        GCA       AOPT
$---------8---------9--------10--------11--------12--------13--------14
        0.18     3702.6     2902.8     2902.8        2.0
```

where,

- EA, EB and EC define the young's modulus in 3 orthogonal directions A, B and C respectively, which represent the material axes. (Definition is mandatory).
- PRBA, PRCA and PRCB represent the Poisson's ratios in the planes BA, CA and CB respectively. (Definition is mandatory).
- GAB, GBC and GCA specify the shear modulus of the material in the planes AB, BC and CA. (Definition is mandatory).
- AOPT is the material axes option.

Since permanent failure is encountered at higher drop height (863.6mm), a material card which is orthotropic but non linear in behavior is defined along with failure strain. This card is very similar to MAT2 card except it has options for defining the stress strain behavior and failure strain. The failure strain obtained from experiments at this drop height is used in this card. The material card number is MAT40 and name of the card is MAT_NONLINEAR_ORTHOTROPIC.

Material properties used for the components are listed in Table 3 and Table 4. Impactor modified density is calculated as shown below.

Mass of the crosshead plates attached to the impact assembly is 2.37 kg

Mass of other assembly components like threaded neck etc., is 0.72 kg

Total mass of the impact load assembly is 3.09 kg.

Actual volume of impactor during experiments is 29922.8 mm^3

$$\begin{aligned} \text{Density} &= \text{mass/volume} \\ &= 3.09/29922.8 \\ &= 1.03e\text{-}^{4}\ \text{kg/mm}^3 \end{aligned}$$

The above numerical value represents the density of the entire impact drop assembly in experiments. In FE model the entire geometry of the impact assembly are not modeled. Instead, the density of the impactor is increased to correspond to the total mass of the drop-weight assembly. This change allows simplifying the model without sacrificing accuracy as impact is a local phenomenon.

The volume of the impactor is reduced in FE model, hence the adjusted density becomes,

Actual volume of the impactor in FE model is 5158.65 mm^3

Volume ratio = (Volume of impactor during experiments) / (Volume of impactor in FE model)

= 29922.8 / 5158.65

= 5.80

Using the volume ratio the adjusted mass and density is calculated as shown in Table 6.1.

Table 6.1: Adjusted mass and density values for impactor

Cases	Density (kg/mm^3)	Volume (mm^3)	Mass (kg)
In Experiments	1.03e-4	29922.8	8.04e-3
FE Model	1.03e-4	5158.65	1.38e-3
Adjusted Values using the volume ratio	1.56e-6	5158.65	8.01e-3

Flexural modulus of elasticity obtained from experiments for each drop height is used in FEA. Poisson's ratio is measured from tensile testing as described in Chapter 2, is used in FEA to define the properties in one direction. Other mechanical characteristics, which are not measured in this work, are obtained from Berman et al. [30] as shown in Table 6.2. Material properties of steel are defined for impactor and support as shown in Table 6.3.

Table 6.2 Material properties of the circuit board (ARL)

Density (kg/mm^3)	Poisson's Ratio	Flexural Modulus (N/mm^2)	Modulus of Rigidity (N/mm^2)
1.763e-7	$\gamma_{xy} = 0.14$	Ex=23650	Gxy = 3702.6
	$\gamma_{yz} = 0.18$	Ey=23650	Gyz = 2902.8
	$\gamma_{zx} = 0.18$	Ez=9101.4	Gxz = 2902.8

Table 6.3: Material properties for impactor and support

Component	Density (kg/mm^3)	Young's Modulus (N/mm^2)	Poisson's Ratio
Impactor	1.56e-6	2.1E2	0.3
Support	7.85E-06	2.1E2	0.3

6.7 Contact Algorithms

The FE models comprise of more than one component, hence contact definitions are needed to be defined between interfering parts. In the dynamic experiment, there are two contacts involved. One contact will be between the lower surface of the board and the support, as the board rests on the support. Other contact will be between the upper surface of the board and the impactor, as the impactor imparts load to the board. These two contacts are incorporated in the FEA using contact definitions in LS-DYNA. Relative motion between the three components is allowed.

Contact between the upper surface of the circuit board and the lower portion of the impactor is incorporated using the "CONTACT_SURFACE_TO_SURFACE" card in LS-DYNA. The same card is also used for establishing contact properties between lower surface of the board and support. Contact between all these components is established using part option. Coefficient of friction of 0.3 between the board and the impactor is also included in this contact card. The Contact card is shown below:

```
*CONTACT_SURFACE_TO_SURFACE
$-------1--------2--------3--------4--------5--------6--------7--------8
     SSID      MSID     SSTYP     MSTYP    SBOXID    MBOXID       SPR       MPR
        1         2

       FS        FD        DC        VC       VDC    PENCHK        BT        DT
      0.3       0.3
```

- SSID indicates the slave segment ID representing the slave surface of the part in the contact.
- MSID indicates the master segment ID representing the master surface of the part in the contact.
- FS and FD are coefficient of static and dynamic friction respectively [13]. Default is 0.0.

There are different methods in which the slave and master surfaces can be defined. SET_SEGMENT is one such option in which the nodes and elements which form the contact surfaces are defined as set segments and the set segment is given a unique identification number. That number is used as SSID or MSID. The other methods by which slave and master surfaces can be defined are by defining the part which forms the contact surface or by defining a BOXID. Box is a 3 dimensional region defined by X, Y and Z coordinates. The defined box is given an ID and it is used in the contact card.

6.8 Boundary Conditions

Two sets of boundary conditions are defined for the FE models. First set deals with the constraints applied on the bottom surface nodes of the support and the second set comprises of the load definition to the impactor as it is defined to move only in the direction normal to the surface of the circuit board.

6.8.1 Constraints

The nodes along the bottom plane of the support are constrained as shown in Figure 6.8. The LS-DYNA card used to define constraints is *BOUNDARY_SPC_NODE. This card has the option of constraining a specified node or a set of nodes along the six degrees of freedom (three translational along the three coordinate axes x, y and z, and three rotational about these axes). Below is a sample of this card defined in the LS-DYNA input file,

```
*BOUNDARY_SPC_NODE
$-------1--------2--------3--------4--------5--------6--------7----------8
 NID/NSID       CID      DOFX      DOFY      DOFZ     DOFRX     DOFRY      DOFRZ
    22200         0         1         1         1         1         1          1
```

- NID/NSID NID is node ID and NSID is node set ID. Hence a specific node or a set of nodes can be constrained using this card.

- DOFX is the degree of freedom in direction X .1 means it is constrained in that direction and 0 means it is not constrained.
- DOFRX is the Rotational degree of freedom in about X axis.

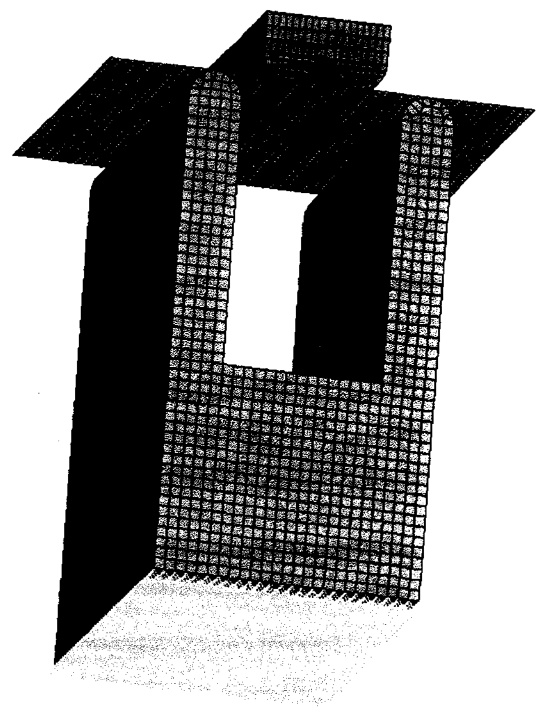

Figure 6.8: FEA model with the base nodes fixed

6.8.2 Load Application

An initial velocity is defined for all nodes of the impactor using "INITIAL_VELOCITY" card in LS-DYNA as shown in Figure 6.9. Below is the sample of this card defined in Ls-Dyna.

```
*INITIAL_VELOCITY
$HMNAME LOADCOLS        1Initial Velocity
$HMCOLOR LOADCOLS        1        3
$---------1---------2---------3
$       NSID    NSIDEX      BOXID
           1         0
$---------4---------5---------6---------7---------8---------9
$         VX        VY        VZ       VXR       VYR       VZR
                         -162.05
```

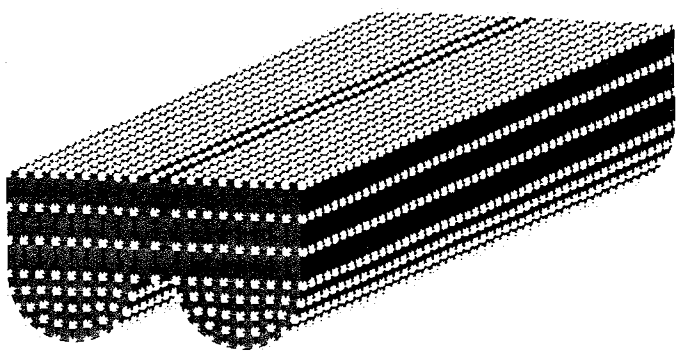

Figure 6.9: Impactor model defined for initial velocity

The initial velocity is calculated as follows:

$$V = \sqrt{2gh}$$

where, g is the gravitational force and h is the drop height of the impactor. The initial velocities calculated are listed in Table 6.4.

Table 6.4: Initial velocities defined in FEA

Drop Height (mm)	76.2	152.4	863.6
Initial Velocity (mm/sec)	1222.72	1729.2	4116.3

6.9 Model Run Time

As stated in earlier chapters, experimental testing of four-point bending by impact is conducted. The test specimen is mounted with gages at the center to measure the strain induced in the electronic board due to bending. The strain data reported is limited to 5 ms from the start of the experiment and to the end. To compare the FE results the test is simulated for 5 ms of run time for the lower drop heights. For the higher drop height, simulation automatically stops as soon as the center element reaches the failure strain.

6.10 Results

The three experiments are simulated in LS-DYNA. The FEA of impact problem is modeled by incorporating all necessary cards in LS-DYNA to model it close to the real experimentation. During the test, the impactor is pushed towards the plate, the force in the form of initial velocity is transmitted to the board through the contact between impactor and the board. Strain is extracted from the center of the board (corresponding to central location in experiment) using the "DATABASE_HISTORY_SHELL" card in LS-DYNA. The time interval for output request is maintained same as the corresponding time interval for the experiments which is 5ms.

Comparison of experimental results with the corresponding FEA results is shown in Figure 6.10 through Figure 6.15. Current models on an average take approximately 3 hrs for the simulation. Overall, FEA results closely match experimental ones, especially in the first half of the motion.

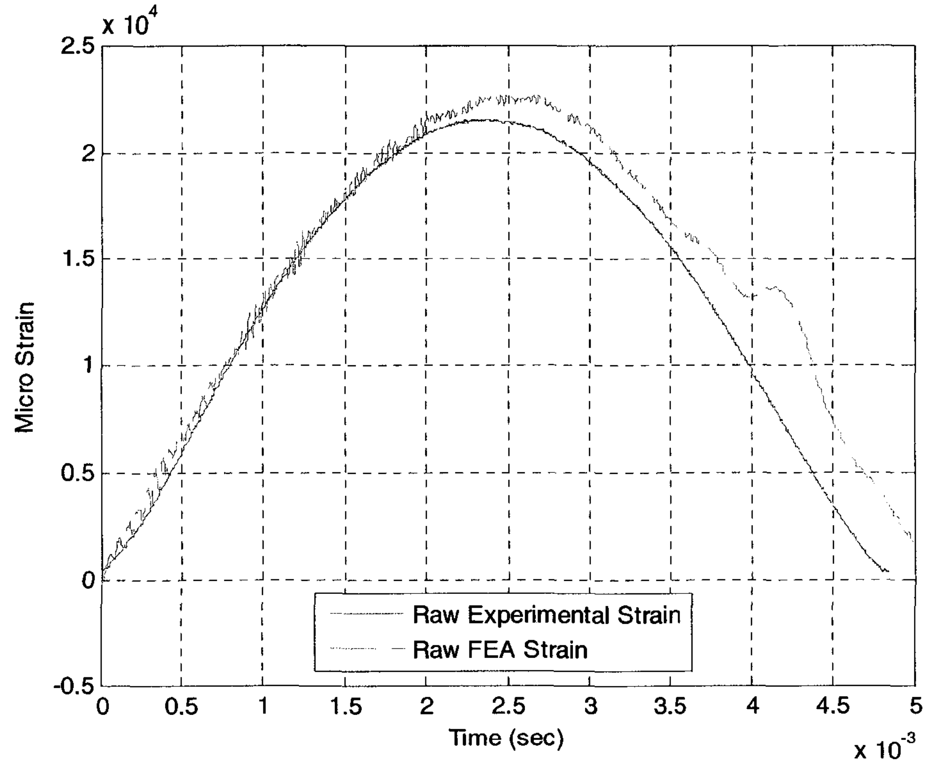

Figure 6.10: Comparison of FEA and experimental strain at drop height 76.2mm

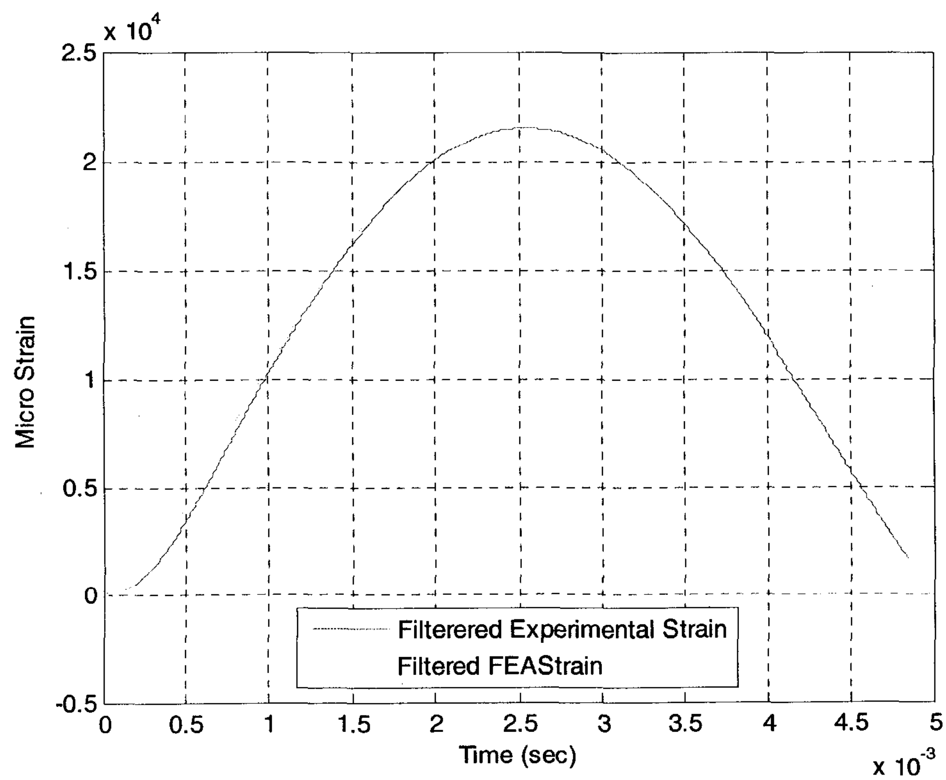

Figure 6.11: Comparison of filtered results at drop height 76.2mm

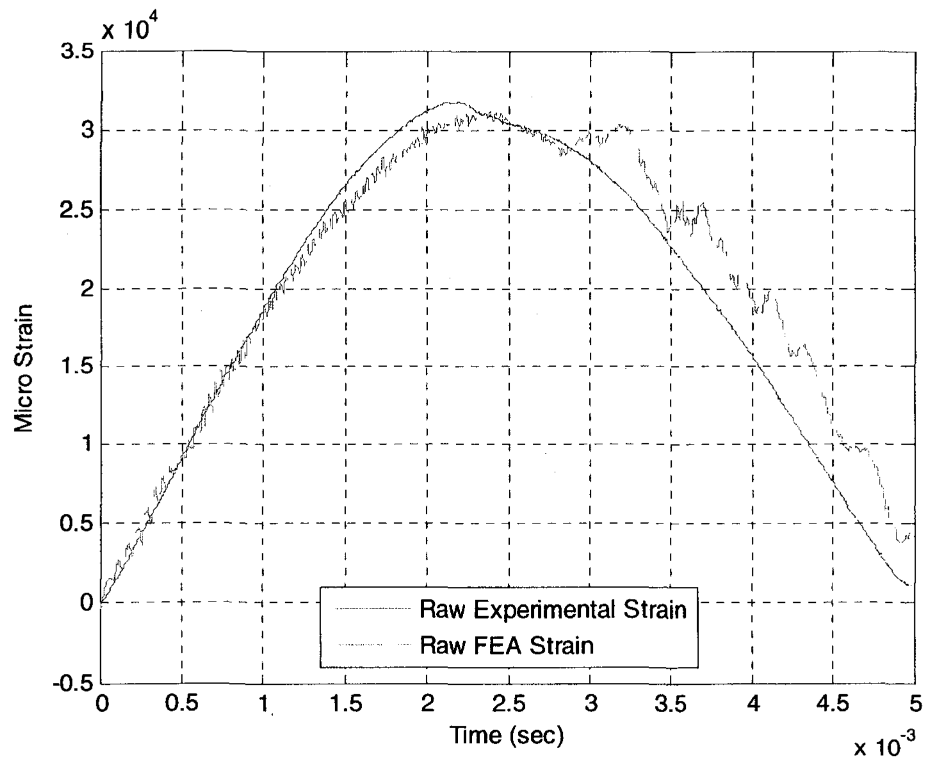

Figure 6.12: Comparison of FEA and experimental strain at drop height 152.4mm

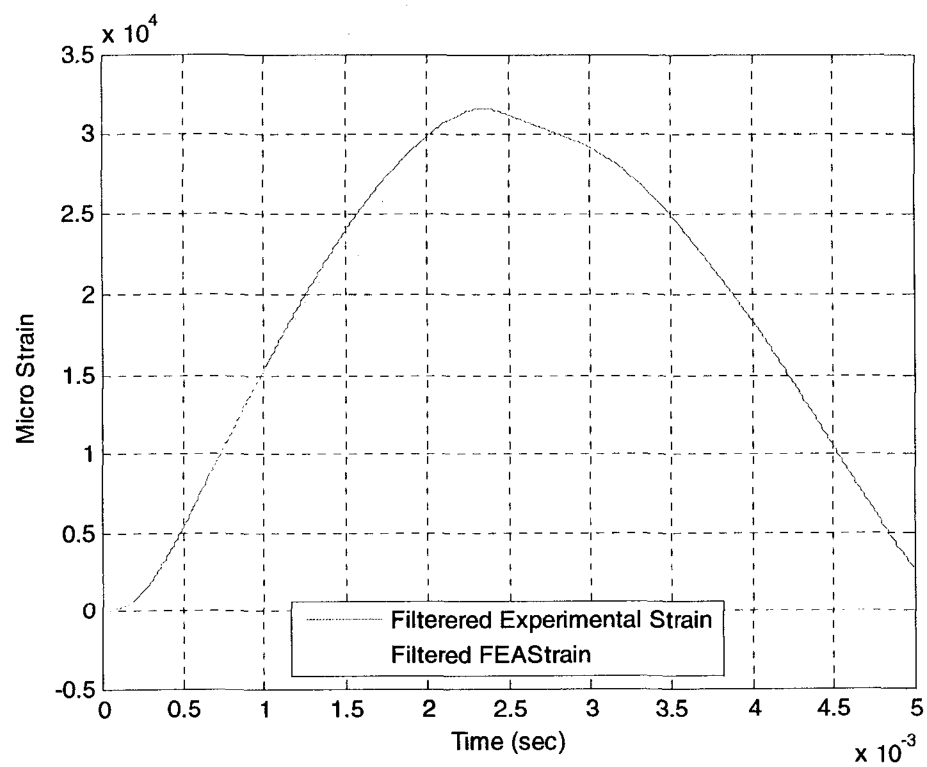

Figure 6.13: Comparison of filtered results at drop height 152.4mm

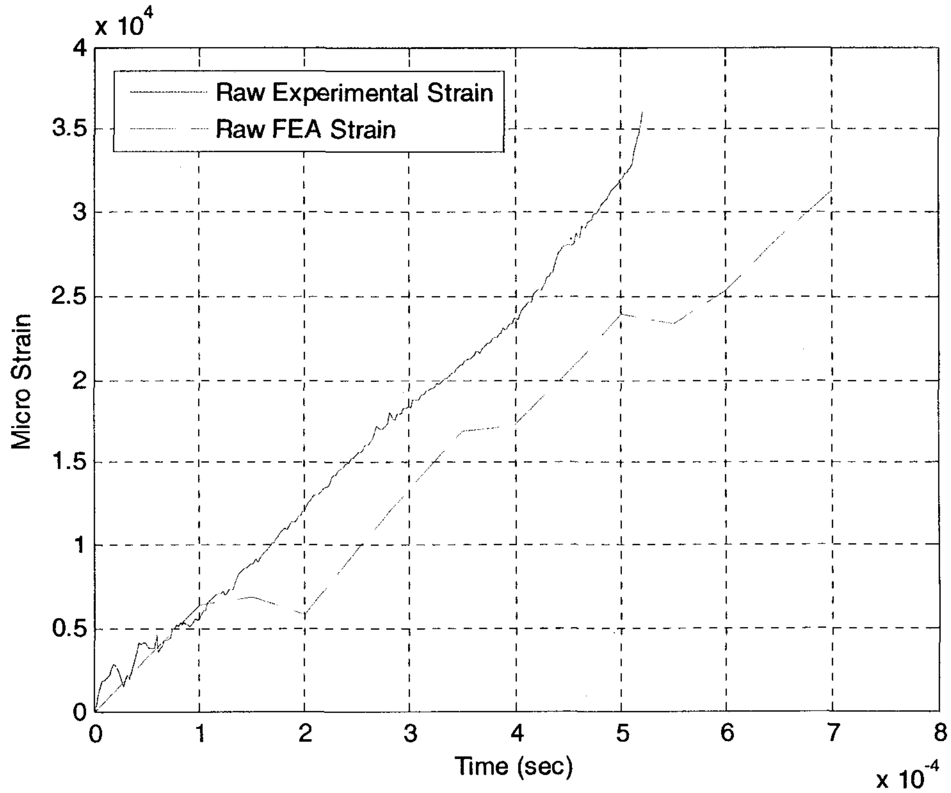

Figure 6.14: Comparison of FEA and experimental strain at drop height 863.6mm

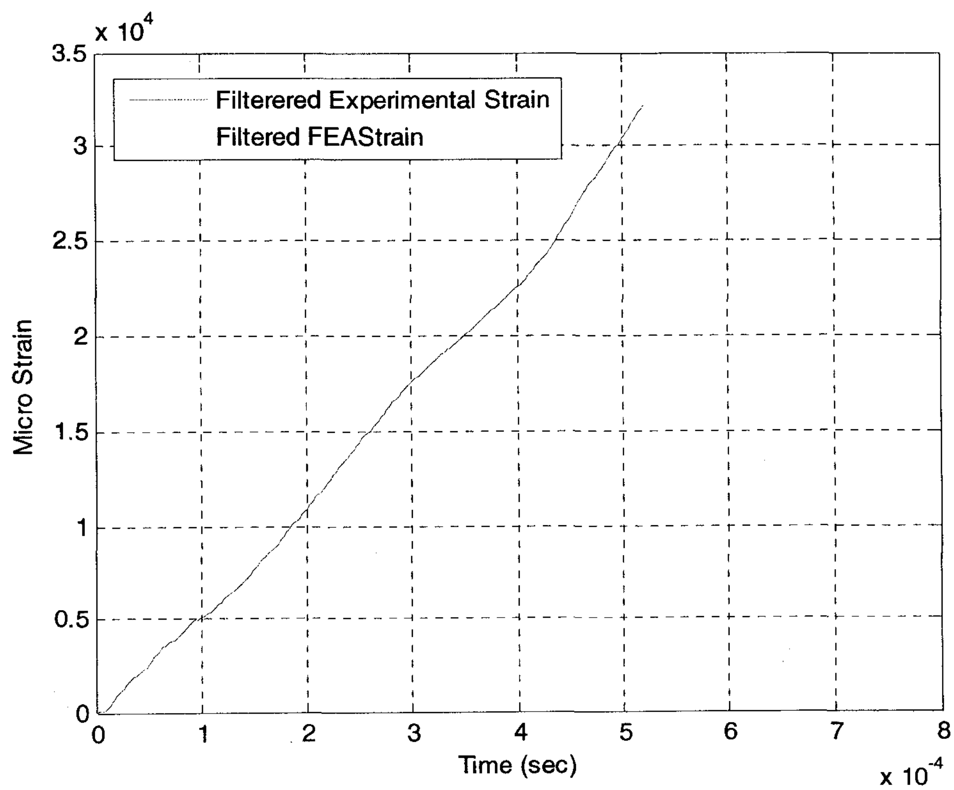

Figure 6.15: Comparison of filtered results at drop height 863.6mm

CHAPTER 7

SUMMARY AND CONCLUSIONS

The last chapter of this thesis compiles the summary of the research performed, observations from axial testing & impact testing of electronic blank boards and recommendations for future work that would build on this research are discussed.

7.1 Research Summary

The objective of this research is to assess the material properties of electronic circuit boards under tensile and impact loading. Four point bending fixture based on ASTM standards is used to measure the material properties under different strain rates. Experiments are conducted in both quasi-static axial and dynamic testing, to study the behavior of the board under different strain rates. MTS machine is used for the axial testing and Dynatup drop weight tower is used for the dynamic range of experiments. Strain gages are used to capture the response of the circuit boards from lower to higher strain rates using signal conditioner and oscilloscope. A total of six different strain rates are achieved successfully, out of which three are in the quasi-static axial testing and three are in dynamic testing. A proper approach for data analysis is proposed to calculate strain rate and Young's modulus of elasticity. Modeling of the four point bending close to the experimental situation using FEA is carried out and simulation results are compared with experimental results. Impact testing is performed to study sensitivity of board materials to strain rates. This research will contribute in understanding the survivability of electronic boards subjected to shock environment under real time conditions.

7.2 Observations from Experiments

- Strain in lateral and longitudinal directions is measured using a 0-90 degree tee rosette, which is used to calculate Poisson's ratio.
- Poisson's ratio does not change with increase in the strain rate during axial testing of electronic boards.
- Tensile modulus of elasticity of boards remains constant around 21 KN/mm^2 under different strain rates tested along the axial direction of electronic boards.
- Tensile strength of electronic boards is found to vary around 290 N/mm^2 during the axial testing which is found from stress strain curve.
- Shock pulses measured in drop weight impact tower are consistent.
- During the impact testing, flexural modulus of elasticity of boards is found to be constant under most strain rates except there is decrease in modulus for the highest strain rate achieved at maximum drop height.
- Failure of the board is observed at 863.6 mm drop height at a strain rate of 60 mm/mm/sec.
- Actual mass of the impact assembly is used in FEA to model the experimental situations accurately.
- FEA of electronic board exhibit close correlation with experimental results on the assumption that electronic board behaves as orthotropic material.

- Shell elements can be used in modeling the circuit board, which will help in reduction of computational time.

7.3 Future Work

- Study behavior of boards at higher drop heights, which yields higher strain rates.
- Study the behavior of boards with different types of electronic components under quasi-static and dynamic conditions.
- A bigger test fixture can also be considered to study the material behavior of electronic boards of different sizes at varying strain rates.
- Each board is tested for one time shock load; it might be interesting to study the behavior under repeated shock loading.
- The sampling size can be increased to have better confidence in the results.
- Flexural modulus of elasticity can be calculated by using 90 degree tee rosette gage for impact loading. This may provide better understanding of variation of the stiffness in two directions during impact bending. These values can be used in defining the orthotropic material properties for electronic board in FEA.
- An approach for modeling of boards with electronic components is presented which can be effectively used to understand the stiffness contribution from the electronic components placed on the circuit boards.

REFERENCES

[1] Rudolph, J. Scavuzzo, and Henry, C. Pusey, "Naval Shock Analysis and Design," Booz-Allen and Hamilton, Inc, 2000.

[2] Heaslip, G., and Punch, J., 2003, "Analysis of Experimental Shock and Impact Response Data of a Printed Wire Board," American Society of Mechanical Engineers, Electronic and Photonic Packing, EPP, Vol. 3, pp. 125-133.

[3] Lim, C. T., and Low Y. J., "Investigating the drop impact of Portable Electronic products," Electronic Components Conference, pp. 1270-1274, 2002.

[4] "ASTM D 3039-76" (Re-approved 1989), Standard test method for tensile properties of fiber - resin composites, Approved Aug. 27, 1976, Published October 1976, Annual Book of ASTM Standards, pp. 118±122.

[5] Okoli OI, Smith GF. "The effect of strain rate and fiber content on the Poisson's ratio of glass/epoxy composites". Compos Struct 2000;48:157–61.

[6] Fayad, G.N., Dagher, H.J., Lopez-Anido, R, Thompson, L., Hess, P.E. "Probabilistic finite element analysis of ASTM D3039 tension test for marine grade polymer matrix composites", International SAMPE Symposium and Exhibition (Proceedings) 50, pp. 1559-1573.

[7] Thota, J., 2006, "Material Characterization and Parametric Studies of Explosion-Proof Vessel," Department of Mechanical Engineering, University of Nevada, Las Vegas.

[8] "JEDEC Standard JESD22-B 104-B", Mechanical Shock, 2001.

[9] Suhir, E., 1992, "Nonlinear dynamic response of a printed circuit board to shock loads applied to its support contour," Journal of Electronic Packaging, Transactions of the ASME, Vol. 114, Issue 4, pp. 368-377.

[10] Varghese, J., Dasgupta, A., 2003, "Test methodology for impact testing of portable electronic products," American Society of Mechanical Engineers, Electronic and Photonic Packaging, EPP, Vol. 3, pp. 71-77.

[11] Goyal, S., Buratynski, E., "Methods for Realistic Drop Testing: International Journal of Microcircuits and Electronic Packaging," Vol. 23, Nov 1, 2000.

[12] Lim, C. T., Ang, C. W., Tan, L. B., Seah, S. K. W., Wong, E. H., “Drop Impact survey of Portable Electronic Products,” Electronic Components and Technology Conference, 2003.

[13] Yu, Q., Kikuchi, H., Ikeda, S., Shiratori, M., Kakino, M., Fujiwara, N., “Dynamic Behavior of Electronic Package and Impact Reliability of BGA Solder Joints,” Proceedings of the Intersociety Conference on Thermal Phenomena, 2002.

[14] Juso, H., Yamaji, Y., Kimura, T., Fujita, K., Kada, M., “Board Level Reliability of CSP,” Electronic Components and Technology Conference, 1998.

[15] Varghese, J., Dasgupta, A., “Test Tailoring Methodology for Impact Testing of Portable Electronic Products,” Proceedings of IMAC-XXI Conference on Structural Dynamics, 2003.

[16] Suhir, E., 2002, “Could shock tests adequately mimic drop test conditions?,” Journal of Electronic Packaging, Transactions of the ASME, Vol. 124, Issue 3, pp. 170-177.

[17] Varghese, J., Dasgupta, A., “Failure Site Transition During Drop Testing of Printed Wiring Assemblies,” Proceedings of ASME InterPACK Conference, 2005.

[18] MIL Standard MIL-STD-883E, Method 2002.3, “Mechanical Shock.”

[19] IEC Standard IEC 60068-2-27, “Environmental Testing-Part 2: Tests, Test Ea and Guidance: Shock.”

[20] JEDEC Standard JESD22-B110, “Subassembly Mechanical Shock.”

[21] Zienkiewicz, O. C., et al., 1991, The Finite Element Method, 4th Ed., Vol. 2, McGraw Hill, New York.

[22] Bathe, K-J., 1996, Finite Element Procedures, Prentice-Hall.

[23] Wong, E. H., “Dynamics of Board-Level Drop Impact,” Journal of Electronic Packaging, 2004

[24] Carroll, D., Zampino, M., and Jones, K., "Bending Simulation of BGA SMT Assemblies and Application to System Level Drop Simulation," Proceedings of ASME IPACK, 2005.

[25] Seah, S.K.W., Wong, E.H., Ranjan, R., Lim, C.T., Mai, Y.-W., 2005, “Understanding and testing for drop impact failure,” Proceedings of the ASME/Pacific Rim Technical Conference and Exhibition on Integration and Packaging of MEMS, NEMS, and Electronic Systems: Advances in Electronic Packaging, Vol. PART B, pp. 1089-1094.

[26] Wu, J., Guosho, S., Yeh, C., Wyatt, K., 1998, "Drop/Impact Simulation and Test Validation of Telecommunication Products," Thermomechanical Phenomena in Electronic Systems -Proceedings of the Intersociety Conference, pp 330-336.

[27] Goyal, S., Papadopoulos, J. M., Sullivan, P. A., "The Dynamics of Clattering II: Equation of Motion and Examples," Journal of Dynamic Systems, Measurement and Control, pages 94-102, 1998.

[28] Varghese, J., Dasgupta, A., "Test Methodology for Impact Testing of Portable Electronic Products," ASME International Mechanical Engineering Congress & Exposition, pages 16-21, Nov 2003.

[29] Shetty, S., Lehtinen, V., Dasgupta, A., Halkola, V., Reinikainen, T., "Fatigue of Chip Scale Package Interconnects Due to Cyclic Bending," Journal of Electronic Packaging, March 25, 2000.

[30] Berman, M., Hopkins, D., Powers, B., and Minnicino, M., 2003, "Numerical and Experimental Modeling of the Transition from Transient to Quasi-static Loading of Printed Wiring Assemblies," SEM Annual Conference and Exposition on Experimental and Applied Mechanics.

[31] Trabia, M., O'Toole, B., Samaan, L., Chakka, K. V., Kuncham, J. V. K., Nallani, G., Sridharala S., Chowdhury, M., 2005, "Finite Element Modeling of Projectile Launch Dynamics," 76th Shock & Vibration Symposium.

[32] Pinfold, M., and Chapman, C., "The Application of Knowledge Based Engineering Techniques to the Finite Element Mesh Generation of an Automotive Body-in-white Structure," Journal of Engineering Design, Vol. 10, No. 4, 1999.

[33] Pinfold, M., and Chapman, C., "Using Knowledge based Engineering to Automate the Post-Processing of FEA Results," International Journal of Computer Applications in Technology, Vol. 21, No. 3, pp. 99-106, 2004.

[34] http://www.expresspcb.com/ExpressPCBHtm/SpecsStandard.htm.

[35] Sridharala. S., 2006, "Material Characterization and Parametric Studies of Explosion-Proof Vessel," M.S. Thesis, Department of Mechanical Engineering, University of Nevada, Las Vegas.

[36] College of Engineering, Montana State University, http://www.coe.montana.edu/ee/jpeterson/Circuit%20Board%20Design.pdf.

[37] Daniel and Ishai, "Engineering Mechanics of Composite Materials".

[38] ASTM Designation D6272, "Standard Test Method for Fexural Properties of Unreinforced and Reinforced Plastics and Electrical Insulating Materials by Four-Point Bending," 2000.

[39] http://www.expresspcb.com/ExpressPCBHtm/SpecsStandard.htm.

[40] http://www.vishay.com/strain-gages/

[41] Vishay Micro-Measurements Instruction Bulletin B-129, Surface Preparation for Strain Gage Bonding

[42] Vishay Micro-Measurements, Strain Gages and Instruments "Application Note TT-605 "

[43] MATLAB: The Language of Technical Computing," 2006, The Mathworks Inc

[44] "Hypermesh User Manual 7.0," 2005, Altair Engineering, Inc.

[45] "LS-DYNA version 970 keyword user's manual," Livemore Software Technology Corporation.

[46] "LS-DYNA theoretical manual," Livemore Software Technology Corporation.

APPENDIX A

UNCERTAINTY ANALYSIS OF EXPERIMENTAL DATA

All experimental measurements are made with a measuring tool or sensor. These tools have a limit to their accuracy. Results from some experiments are calculated from several different measured values. The strength of a tensile specimen is equal to the measured "force" at failure divided by the cross-sectional area of the specimen.. Uncertainty Analysis is the procedure used to determine the propagation of uncertainty when calculating a value like "strength" from multiple measured values.

Kline and McClintock have presented a precise method of estimating uncertainty in experimental results. The method is based on a careful specification of the uncertainties in the various primary experimental measurements. When the plus or minus notation is used to designate the uncertainty, the person making this designation is stating the degree of accuracy with which he or she believes the measurement has been made. It is notable that this specification is in itself uncertain because the experiment is naturally uncertain about the accuracy of these measurements.

If a careful consideration of an instrument has been performed recently, with standards of very high precision, then the experiment will be justified in assigning much lower uncertainty to measurements than if they are performed with a gage or instrument of unknown calibration history. The uncertainties of the results of the experimental works are calculated by using Kline and McClintock Method. The equation used for this method is given below.

$$W_R = \left[\left(\frac{\partial R}{\partial x_1} w_1 \right)^2 + \left(\frac{\partial R}{\partial x_2} w_2 \right)^2 + \cdots + \left(\frac{\partial R}{\partial x_n} w_n \right)^2 \right]^{\frac{1}{2}} \qquad \text{Equation A1}$$

where, W_R = the uncertainty in the experimental results,

R = the given function of the independent variables $x_1, x_2 \ldots x_n$

$R = R(x_1, x_2 \ldots x_n)$

$w_1, w_2 \ldots w_n$ = the uncertainty in the independent variables.

A.1 Uncertainty Calculation for MTS Data

The uncertainty analyses for stress (σ), percentage elongation (%El) are calculated. The stress is based on the load (P) and the initial cross-sectional area (A_i) of the tested specimen. The %El is based on the change in length (Δl) during the testing. The magnitude of P is obtained from the load-cell of the MTS unit. The values for Δl and A_i are calculated based on measurements by a caliper. The uncertainties in load-cell and caliper are ± 0.134 % N and ± 0.0254 mm respectively, obtained from the calibration. The tensile stress is given by the equation,

$$\sigma = P/A_i \qquad \text{Equation A2}$$

A.1.1 Calculation of Uncertainty in Stress (U_σ)

$U_\sigma = U_{(P, Ai)}$

$U_{Ai} = (U_{Di})^2$

Uncertainty in load-cell = ± 0.134 % N

Uncertainty in caliper = ± 0.0254 mm

Sample calculation:

The tensile strength and elongation values from the crosshead speed of 0.0244mm/s are considered for this uncertainty analysis.

For a tensile strength = 273 N/mm^2

The measured load (P) = 4924.2 N

Uncertainty in load (U_P) = 4924.2 × 0.00134

= ± 6.6 N

Uncertainty in cross-sectional area (U_{Ai}) for the tensile specimen:

Uncertainty in measuring width and thickness ($U_{wi} = U_{ti}$) = ± 0.0254 mm.

Cross-sectional Area (A_i) = w*t

= 12.7 x 1 422 mm^2

= 18.1 mm^2

A_i = w*t

Differentiating with respect to width (w),

$$\frac{dA_i}{dw_i} = t$$

= 1.442 mm.

Differentiating with respect to width (w),

$$\frac{dA_i}{dt_i} = w$$

= 12.7 mm

Uncertainty in area, $U_{Ai} = \left[\left(\frac{dA_i}{dw_i} \cdot U_{wi}\right)^2 + \left(\frac{dA_i}{dt_i} \cdot U_{ti}\right)^2\right]^{\frac{1}{2}}$

$$= [(1.442 \text{ x } 0.0254)^2 + (12.7 \text{ x } 0.0254)^2]^{1/2}$$

$$= \pm 0.325$$

Uncertainty in stress, $U_\sigma = \left[\left(\frac{\partial \sigma}{\partial P} \cdot U_P\right)^2 + \left(\frac{\partial \sigma}{\partial A_i} \cdot U_{A_i}\right)^2\right]^{\frac{1}{2}}$ Equation A3

$$\sigma = \frac{P}{A_i}$$

$$\frac{\partial \sigma}{\partial P} = \frac{1}{A_i}$$

$$= 0.0553$$

$$\frac{\partial \sigma}{\partial A_i} = -\frac{P}{A_i^2}$$

$$= -4924.2 / (18.1^2)$$

$$= -15.03$$

Now providing all the numerical values in Equation A3 obtained from the calculation, it is found that,

$$U_\sigma = \left[(0.0553 * 6.6)^2 + (-15.03 * 0.325)^2\right]^{\frac{1}{2}}$$

$$= 4.89 \text{ N/mm}^2$$

Therefore, for a tensile strength 273 N/mm^2 the uncertainty is 4.89 N/mm^2. One example of the use of the uncertainty analysis for tensile stress is shown in this section. This can be implemented to other experimental results discussed in this thesis.

A.1.2 Calculation of Uncertainty in Percentage Elongation ($U_{\%El}$)

<u>Sample calculation:</u>

Gage length (l) = 152.4 mm

%El $= \frac{\Delta l}{l} \cdot 100$

Uncertainty in Δl ($U_{\Delta l}$) $= \pm 0.0254$ mm

Uncertainty in %El ($U_{\%El}$),

$$U_{\%El} = \left[\left(\frac{d\%El}{d\Delta l} \cdot U_{\Delta l}\right)^2\right]^{\frac{1}{2}} \qquad \text{Equation A4}$$

$$\frac{d\%El}{d\Delta l} = \frac{100}{l}$$

$$= 0.66$$

Providing all the calculated values in Equation A4, it is found that,

$$U_{\%El} = \left[(0.66 * 0.0254)^2\right]^{\frac{1}{2}}$$

$$U_{\%El} = \pm 0.017$$

One example of the use of the uncertainty analysis is shown in this section. This can be implemented to all experimental results discussed in this thesis.

APPENDIX B

STATISTICAL ANALYSIS OF EXPERIMENTAL DATA

Statistics is the science of collection, classifying and interpreting data based on the number of samples. As a result, statistics includes the methodology of data analysis. Standard deviation is a commonly used statistical method to find the variation of data points by keeping mean as a reference. The formula for standard deviation is shown in Equation B1.

$$SD = [\sum (x-\mu)^2 / n-1]^{1/2} \qquad \text{Equation B1}$$

where, x = sample value

μ = mean of the sample

n = sample size.

Sample Calculation: Finding the standard deviation for tensile modulus of elasticity.

x 1= 20..7

x 2 = 21.14

x 3 = 21.06

μ = 20.97

n = 3

Plugging in these values in equation 1,

SD = 0.05495

SD = 5.45 %

Similarly, standard deviation calculated for tensile strength is shown in Table B1.

Table B1: Standard deviations for tensile testing

Experimental Variables	Crosshead Speed (mm/sec)			Standard Deviation (%)
	0.0244	0.244	2.44	
Tensile Modulus (KN/mm^2)	20.7	21.14	21.06	5.45
Poisson's Ratio	0.112	0.115	0.114	0.15

One example of the use of the statistical analysis is shown in this section. This can be implemented to all experimental results discussed in this thesis.

VITA

Graduate College
University of Nevada, Las Vegas

Ashok kumar Ayyaswamy

Home Address:
4248 Grove Circle Apt#3
Las Vegas, Nevada 89119

Degree:
Bachelor of Engineering, Mechanical Engineering, 2002
University of Madras

Publications:

"Characterization of Electronic Board Material Properties Under Impact Loading", ASME International Mechanical Engineering Congress & Exposition, 2007, Seattle, Washington.

"Optimization of the structural response of a light-weight composite blast containment vessel by using fuzzy logic", ASME International Mechanical Engineering Congress & Exposition, 2007, Seattle, Washington.

Thesis Title:
Characterization of electronic board material properties under impact loading

Thesis Examination Committee:
Chairperson, Dr. Mohammed Trabia, Ph. D.
Chairperson, Dr. O'Toole, Ph. D.
Committee Member, Dr. Ajit Roy, Ph. D.
Committee Member, Dr. Daniel Cook, Ph. D.
Graduate Faculty Representative, Dr. Samaan Ladkany, Ph. D.